



KA103X DEGREE PROJECT IN ENGINEERING CHEMISTRY
INSTITUTION OF CHEMISTRY
STOCKHOLM, SWEDEN 2021

Photochemistry of Copper Coordination Complexes

Amanda Blad
Helena Glisén
Filippa Ludvig

Fotokemi av kopparkoordinationskomplex

School of Engineering Sciences in Chemistry, Biotechnology and Health

KA103x: Bachelor Thesis in Chemical Engineering

Credit: 15 HP

Supervisors: James Gardner and Suchithra Ashokan Sahadevan

Examiners: James Gardner and Michael Malkoch

June 9, 2021

Abstract

The United Nations have set a number of sustainability goals, Agenda 2030, in order to combat the world's largest challenges and injustices. The energy market is one of these urgent issues which must be solved. Solar energy is expected to be the fastest growing energy source in the future energy market. It can be a great way to provide zero emission energy, but also become a key part in equality as it can provide energy to people who live off the grid today and raise quality of life all over the world.

The aim of this study is to compare different ligands in a copper halide complex to conclude what structural properties of the ligand may be better suited for photoluminescent applications, and especially in solar cells. Eight ligands were chosen for the complexes depending on their level of conjugation: 4,4'-bipyridine, tri(o-tolyl)phosphine, 3,6-di-2-pyridyl-1,2,4,5-tetrazine, pyridine, pyrimidine, pyrazine, phenanthroline, and 2,2'-bipyridine. A series of analytical methods were used to compare the complexes properties; X-Ray diffraction, photoluminescence spectroscopy, time-resolved photoluminescence spectroscopy, microscopy and thermochromism. From these measurements, pyridine and pyrimidine proved to have the greatest potential for working in a solar cell. This was deduced because of the detected crystallinity, having luminescence under UV-light, forming distinct wavelength peaks during excitation and emission in the fluorometer, having the longest excited state lifetime and finally, emitting distinctive colours during thermochromism.

When making the solar cell, pyridine was chosen as ligand due to higher availability than pyrimidine. The method used in this project for making the solar cell is directly applied from a previously tested method, which was designed for another type of electron donor. This project compared the different ways of applying the copper halide complex on to the cell. The methods used were spin-coating and SILAR for creating the copper iodide thin film and vapour diffusion and immersion to introduce the ligand. These four methods were then tried systematically for all combinations. The finished solar cells were put in a solar simulator where voltage, current, efficiency and fill factor was measured. The best results came from the solar cell where spin coating and immersion was used.

Copper halide complexes in previous studies have been proven to be reactive with oxygen and the experiments in this project were not carried out in an inert environment. This could have had significant impact on the measurements, as reactions between the complexes and oxygen may have resulted in oxidation and thus inactivation of the complexes. Therefore, it would be interesting to conduct the syntheses again but this time in an inert environment to determine whether oxygen made a major impact on the measurements. In further studies, it would also be worthwhile to investigate how the different layers of the solar cell would have to be adapted for this particular complex to obtain higher efficiency and voltage. Also, making thin film solar cell with pyrimidine would be valuable since it showed attributes for a solar cell. Furthermore, it would be interesting to use derivatives of pyrimidine, such as uracil and cytosine which are abundant in nature, as they might be more sustainable choices. This is due to their inherent ability to degrade and not posing a threat to either health or environment when handled.

Keywords: Copper Halide Organic Complex, Time-Resolved Photoluminescence, Metal-organic Framework, Coordination Polymer, Thin Film Solar Cell.

Sammanfattning

Agenda 2030 är hållbarhetsmål uppsatta av Förenta nationerna (FN) för att bekämpa världens största utmaningar och orättvisor. Energimarknaden är ett av dessa brådskande problem som måste lösas, och en möjlig lösning på detta är solenergin, som förutspås vara den snabbast växande energikällan i den framtida energimixen. Att utvinna solenergi i form av solceller är ett bra alternativ eftersom det inte producerar några koldioxidutsläpp vid användning, de kan användas av människor som saknar tillgång till ett etablerat elnätverk idag och höja levnadsstandarden som i sin tur främjar jämlikhet i världen.

Syftet med den här studien är att jämföra olika ligander i ett kopparhalidkomplex för att utefter strukturella attribut hos liganden dra slutsatser om vilken komponent som passar bäst i applikationer som kräver fotoluminescens, framförallt för tillämpning i solceller. Åtta ligander valdes utefter deras konjugering för att undersökas. De åtta liganderna är 4,4'-dipyridin, tri(o-tolyl)fosfin, 3,6-di-2-pyridyl-1,2,4,5-tetrazin, pyridin, pyrimidin, pyrazin, fenantrolin och 2,2'-dipyridin. De analytiska metoderna som användes för att jämföra komplexens egenskaper var: röntgendiffraktion, spektroskopi, fotoluminescens, mikroskopi och termokromism. Pyridin och pyrimidin visade störst potential för att användas i en solcell. Egenskaperna som undersöktes var kristallinitet, luminiscens under UV-ljus, livstid av det exciterade tillståndet samt om de emitterade någon färg under termokromism.

Liganden som valdes till att göra ett komplex för en tunnfilmssolcell var pyridin. Metoden att göra solcellen med var beprövad sedan tidigare, men i denna studie användes en annan elektrondonator. Detta projekt jämförde två olika sätt att applicera kopparjodidkomplexet på ett glassubstrat. Metoderna som användes var antingen spin coating eller SILAR, och för att applicera liganden testades ångdiffusion eller nedsänkning direkt i ligand-lösningen. När solcellen var klar mättes elektrisk spänning, ström, verkningsgrad och fyllnadsfaktor. De bästa resultaten kom från att kombinera spin coating och direkt nedsänkning i ligandlösning.

Kopparhalidkomplexen har i tidigare studier bevisats att oxidera i kontakt med luft, vilket kan ha haft en betydande påverkan på resultaten i detta projekt som ej utfördes under inerta förhållanden. För framtida projekt kan det därför vara intressant att utföra samma synteser av komplexen fast i en inert miljö. Andra aspekter kan vara att undersöka huruvida de olika lagren ska vara optimerade för just kopparjodidkomplex för att få bättre resultat. Att undersöka vad pyrimidin och derivat av pyrimidin, så som uracil och cytosin, hade gett för resultat i en solcell hade också varit givande då dessa är bättre alternativ ur hälso-, och miljöperspektiv.

Nyckelord: Koppar halid organiska komplex, tidsberoende fotoluminescens, metallorganiska ramverk, koordinationspolymer, tunnfilmssolcell.

Abbreviations

CuI	Copper(I) Iodide
$\text{CuSO}_4 \cdot \text{H}_2\text{O}$	Copper(II) Sulfate Hydrate
FTO	Fluoride-Doped Tin Oxide
HTM	Hole Transporting Material
KI	Potassium Iodide
MOF	Metal-Organic Framework
N/A	Not Applicable
N/D	Not Determinable
$\text{Na}_2\text{S}_2\text{O}_3$	Sodium Thiosulfate
SILAR	Successive ionic layer adsorption and reaction
TRPL	Time-Resolved Photoluminescence
UV-Vis	Ultraviolet-Visible spectroscopy
V_{OC}	Voltage Open Circuit
XRD	X-Ray Diffraction

Contents

1	Introduction	1
1.1	Copper Halide Organic Complexes	1
1.2	Structural Attributes Affecting Electrical Conductivity	2
1.3	Experimental Techniques	3
1.3.1	Spin coating	3
1.3.2	SILAR method	3
1.3.3	Ligand Application	3
1.4	Thin Film Solar Cell	3
1.5	Analytical Techniques	4
1.5.1	X-Ray Diffraction	4
1.5.2	UV-Vis Spectroscopy	4
1.5.3	Time-Resolved Photoluminescence Spectroscopy	4
1.5.4	Thermochromism	5
1.6	Aim	5
2	Methods	6
2.1	Laboratory Method for Powder Synthesis	6
2.1.1	Microscopy	6
2.1.2	X-Ray Diffraction	7
2.1.3	Photoluminescence Spectroscopy	7
2.1.4	Time-Resolved Photoluminescence Spectroscopy	7
2.2	Laboratory Method for Thin Film Solar Cell Synthesis	7
2.2.1	Copper Iodide Organic Complex Application	8
2.2.2	Current-Voltage Measurements	8
3	Results	9
3.1	Powder Results	9
3.1.1	Crystal Structures	9
3.1.2	Excitation and Emission Wavelengths	10
3.1.3	Time-Resolved Photoluminescence Equations	10
3.1.4	Thermochromism	11
3.2	Solar Simulation Measurements	11
4	Discussion	13
5	Conclusion	15
6	Appendix	18

1 Introduction

Future climate change challenges continues to grow as carbon-, and fossil-based fuels are still used as the worlds primary energy resources. An alternative to these types of energy sources, and in accordance with the Agenda 2030 sustainable development initiative formed by the United Nations, this report will explore a possible approach to making sustainable solar cells. To provide sustainable energy, a larger diversification in the energy marked is needed. Today, solar cells are under represented and therefore research and further expansion is demanded.

As of today, there are millions of people living without access to electricity and clean energy. This must change in order to minimize socioeconomic divides and elevate living standards within outlying communities. Solar power has the potential to provide multiple communities with clean electricity permanently, without having to wait for national electricity grids to be developed [1]. The expansion of solar power is expected to grow all over the world steadily in near future, and has been calculated to represent 60 % of the renewable energy expansion capacity in 2025 [2].

When the solar power demand grows, so does the production of solar cells. In this report, further development of a new kind of solar cell has been investigated by exploring the photoluminescent properties of copper halide organic complexes. The created solar cell could be a more sustainable choice than today's existing solar cells by using more earth abundant materials than other renewable energy technologies currently does.

1.1 Copper Halide Organic Complexes

Charge transfer bands occurs when an electronic transition takes place between orbitals that are centered on different atoms. These transitions follow the governing rules for excitation, hence the electronic transition is allowed. Charge transfer can happen metal to ligand, ligand to metal, metal to halide, halide to metal or between metal atoms if they are directly bound to each other. When the electron density shifts in the complex during the electronic transition, it gives rise to intense absorption and gives off strong colour. This is of interest when studying copper halide organic complexes, as the structure of these complexes allows for one or multiple of these transitions to take place. Due to their high probability of having photoluminescent properties, copper halide organic complexes are therefore suitable for electrical applications [3]. The ligands which will be used for this project are 4,4'-bipyridine, tri(o-tolyl)phosphine, 3,6-di-2-pyridyl-1,2,4,5-tetrazine, pyridine, pyrimidine, pyrazine, phenanthroline and 2,2'-bipyridine. The skeletal structures of the ligands are shown in Figure 1.

For this study, the metal halide core used in the complexes is copper iodide. A potential problem is that the copper halide is very reactive with oxygen in the air, creating an unwanted product. A larger halide is less reactive than a smaller halide. For instance, iodine is larger than fluorine, chlorine and bromine, and is therefore less reactive. The reactivity is related to the valence electrons, as they possess higher energy in a smaller halide. The valence electrons in iodine are higher and the atom itself does not gain as much stability by sharing a pair of valence electron in comparison to fluorine, chlorine and bromine. By utilizing iodine in the complexes, it is meant to minimize this particular problem [4]. Although, it is worth mentioning that in previous studies, there seems to be no significant difference with electrical transfer within the complex when creating a copper complex of iodine, bromine or chloride [5]. Therefore, there are only advantages of using iodine since the experiments have been performed in conditions where the copper complex is more reactive [4].

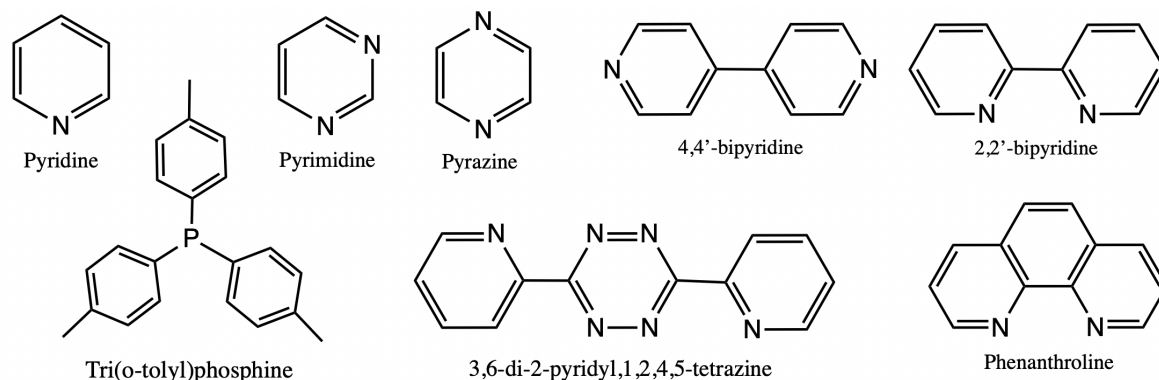


Figure 1: Structures of ligands used for this project.

1.2 Structural Attributes Affecting Electrical Conductivity

When analyzing the created complexes, there will be a number of structural attributes which influences the fluorescent properties of the complexes. This study is limited to how the effects of conjugation and crystallinity affects the material.

A conjugated system consists of p-orbitals with delocalized electrons. These p-orbitals must be parallel to each other, i.e. in phase. This allows for the orbitals in phase to overlap, and the delocalized electrons can move between the orbitals. Typically, alternating sigma-bonds and pi-bonds create conjugation between two atoms but carbenium ions, radicals and lone pairs are also able to participate to create a conjugated system as they all have the required p-orbitals.

In metal-organic frameworks (MOFs), such as copper halide organic complexes, incorporating ligands consisting of chelating groups have created extended conjugated systems over both the inorganic and organic components. The conjugation within the ligand can contribute to the charge delocalization within the molecule, while the charge transfer between ligand and d-block metal is suspected to be the dominant mechanism behind the materials conductivity [6]. In a study published in 2016, it was investigated how increasing pi-conjugation effected the efficiency in ferrocene based dye sensitized solar cells. It was concluded that larger conjugated systems had a higher power conversion efficiency than smaller ones, though the power conversion of the materials studied were overall low [7]. Another study found that conjugation had a great impact on the efficiency in photovoltaic applications, but that more aspects such as intermolecular aggregation needs to be accounted for when designing a solar cell [8]. In addition, another study has reported that extending the light-harvesting capability of copper halide complexes into the red part of the electromagnetic spectrum by increasing the conjugation of the organic ligand proves to increase the efficiency of the complex [9]. Therefore, it is essential to examine whether the size of the conjugated system in the ligand may have an impact on the overall photoluminescent properties of the copper coordination complex.

MOFs have traditionally not been observed to have a high electrical conductivity and only recently a greater interest has been formed concerning their electrical properties. MOFs can consist of an endless variety of both metal cores and ligands, and may provide many opportunities for crystal design as the coordination polymer of copper coordination complexes can be built in one-, two-, and three-dimensional structures [6].

The produced MOFs are expected to have crystalline structures, and the electrical conductivity is suspected to greatly depend on the crystallinity of the material. A crystalline structure allows for a greater free mean path for electrons, as a regular periodic lattice allows for the single wave functions of atoms to combine and make one electric wave function for the entire lattice. This is in line with Bloch's Theorem, which can be used to describe the state of electrons in crystalline solids [10]. If the MOF instead would be amorphous, the single electron wave functions would not be able to combine as efficiently and extend through the lattice. If the MOF would be partly amorphous and partly crystalline, the wave functions for the electrons would be able to partly combine, but not throughout the entire material. Crystallinity

may therefore have a considerable impact on the charge carrying properties of the complexes, and be a key component when deciding whether or not a certain complex is suitable for electronic applications.

1.3 Experimental Techniques

This section describes the different methods for application of the copper iodide and ligand onto the substrate that will later become the finished solar cell. The methods that will be described are: spin coating, SILAR-method, vapour diffusion and immersion.

1.3.1 Spin coating

Spin coating is a technique used for applying thin films of compounds to substrates. The substrate is placed in a spin coating machine and the desired coating material is added. By spinning the solvent covered substrate at a high speed, it is possible due to the centripetal force and the surface tension of the solvent to obtain an even film on the substrate surface. Spin coating can be repeated several times to build a desired thickness of the thin film, and the usual thicknesses of the films created by spin coating ranges between nanometers to microns [11].

1.3.2 SILAR method

Successive ionic layer adsorption and reaction (SILAR) is another method utilized to deposit compound materials on substrates. The method consists of a cycle with four steps; dipping the substrate in a liquid containing anions, then deionized water, a liquid containing cations and finally deionized water again. This is repeated a certain amount of times, for a certain amount of cycles. The principle of the method is the cycling between different ions. After desired amount of cycles, a thin film of the product will have formed on the substrate. The thickness of the film can be fine-tuned by adjusting each immersion time in the liquids, or by changing the amount of cycles. SILAR can be carried out at room temperature which prevents oxidation that typically accompany processes at higher temperature, and is suitable for covering larger areas [12].

1.3.3 Ligand Application

The application of a ligand onto the substrates is either done by vapour diffusion or immersion. The vapour diffusion method is used to form a homogeneous film. Vapour diffusion is used after the SILAR method or spin coating. Its purpose is to introduce the the ligand in a gaseous state to the substrate with the intention of forming a product on the surface. The ligand liquid must be volatile in order for the ligand to enter the gas state and reach the copper iodide surface. In immersion, the ligand is introduced by simply immersing the substrate into the ligand solution [13].

1.4 Thin Film Solar Cell

The method used for creating the thin film solar cell is from a report by Sadollahkhani et al. [14]. The only difference between the method that will be applied in this project to the original method is that the light absorbing material will be the copper halide organic complex instead of a perovskite structured material. As mentioned before, the copper halide organic complexes are somewhat unstable, similar to the perovskite solar cell. The copper halide organic complex is unstable when in proximity to oxygen, while the perovskite cell is easily soluble in solutions, for instance water. In previous studies there are two ways of approaching this problem. A physical barrier for the cell would impede the oxygen from entering the cell. Another solution is to rework the material to its surroundings by adding new functional molecules and make the complex less reactive. A protective layer for a solar cell could be a hole transport material layer (HTM-layer) since it is the topmost layer that covers whole exposed cell. In this study, the HTM-layer is however made specially for a perovskite structured material as electron donor, and not for a ligand [15].

1.5 Analytical Techniques

In the following section, the theory behind the practised analytical techniques will be presented. The use of each analytical method will be motivated, and the data gathered from each analytical method will be explained.

1.5.1 X-Ray Diffraction

X-Ray diffraction (XRD) is an analytical characterization technique utilizing a monochromatic light source for crystalline material characterization. The method provides structural information such as crystal orientations, distance between lattice planes and the ratio between crystalline and amorphous regions. XRD spectra have specific peaks for the compound being analyzed and these peaks are equivalent with a given materials atomic arrangement. Through Bragg's law, in equation 1.1, which describes how light is diffracted in a crystal, it is possible to determine the distance. n is the integer, λ is the wavelength, d is the distance between the lattice planes from the corresponding angle of the measured peaks in the spectra and θ is the angle.

$$n \times \lambda = 2 \times d \times \sin\theta \quad (1.1)$$

From the distance between the lattice planes, the Miller indices can be determined which describes the intercepts in the crystal planes. This can be further used to determine the crystal family and structure for an analyzed compound [16] [17].

1.5.2 UV-Vis Spectroscopy

Spectroscopy is an analytical method where radiation is absorbed, emitted or shifted in frequency after interaction with a material. The technique is applicable for a variety of compounds and suited for measurements when the change of absorbance is only correlated to the wavelength [18].

The sample is exposed to a light source, and an absorbance spectrum for the sample is obtained. The data received gives qualitative and quantitative information about the sample. The peaks of an absorbance spectrum are specific for the analyzed compound and the area underneath the peaks is equivalent to the concentration. Through this measurement, one can obtain the wavelengths where absorbance within the compound occurs. As the wavelength for maximum absorbance often coincides with the wavelength for maximum excitation of a species this is a simple technique to investigate possible wavelengths which can excite said species. By noting the observed wavelength and using it in photoluminescence spectroscopy, one can refine the results and obtain the maximum wavelengths for both excitation and emission. Furthermore, when these values are known they can be used in time-resolved photoluminescence spectroscopy to determine how the intensity of an excited state decays over time for a compound [19].

1.5.3 Time-Resolved Photoluminescence Spectroscopy

Photoluminescence Spectroscopy is an optical characterization technique where a spectrum is obtained by measuring the intensity of emitted radiation from a compound. Depending on whether the emitted radiation is a function of the excitation or emission wavelength, different spectrum can be derived [20]. Fluorescence measurements are typically divided into two different types of measurements. These types are steady-state measurements and time-resolved photoluminescence measurements. For this project, only time-resolved photoluminescent measurements are used. Time-resolved photoluminescence measurements are used for measuring intensity decays, and can be utilized when observing the decay of excited electronic states. The decay of excited states are usually rapid, within nanoseconds for fluorescent compounds and milliseconds to seconds for phosphorescent compounds, which craves spectroscopy tools that can detect changes within small time-frames. In time-resolved photoluminescence measurements the sample is exposed to a short pulse of light which excites the sample and the decay in intensity over time can be measured. The decay in intensity over time is describes in equation 1.2.

$$I(t) = I_0 \times e^{-t/\tau} \quad (1.2)$$

In equation 1.2 which describes the decay of an excited state, I_0 is the intensity at $t = 0$, t is the time and τ is the single decay time. In reality however, the intensity of a measured compound sometimes must be described by more than only one exponential equation which could be due to factors within the molecules such as anisotropy decay. For this project, an assumption has been made that the decay of the synthesized complexes can be described by a linear combination of two exponential functions. One component describes the initial fast decay of the excited state and the other component describes the slower part of decay of the excited state [21].

There are many processes occurring within the nanoscale time frame which can affect the lifetime of a fluorophore, such as photoinduced electron transfer, energy transfer and reorientation. These processes are typically referred to in a more general term as quenching processes. For the thin film solar cell, it is beneficial to have a rapidly decaying excited state as this indicates that a quenching process has taken place. On the other hand, the excited state must also be long enough for the desired electron transfer reaction to occur before the complex has returned to its ground state. For this project, the type of quenching that would ideally take place is a photoinduced electron transfer, which means that a charge separated electron-hole pair has been created. The electron is then excited to the conduction band while leaving a hole in the valence band. If this happens in a compound which is connected to an external circuit, the electrons can move to the negative terminal and the holes can move to the positive terminal. Moving charges to the different terminals induces a current, and thus electricity has been created. This means that the faster the decay of the induced excited state, the more electron-hole pairs have been generated thus more charge can be recovered and turned into electricity.

The results from the time-resolved photoluminescence spectroscopy should ideally give a rapidly decaying first component, as this is more promising for application of the analyzed complex in a thin film solar cell. Though, it should be noted from earlier that other processes can take place were the molecule is returned to its ground state which are not promising for photovoltaic applications. This process includes both emissive and non-emissive processes such as vibrational relaxation, internal conversion, intersystem crossing, collisions and heat dissipation. Therefore, a rapidly decaying excited state may not be directly linked to having a great potential in photovoltaic applications [22] [23].

1.5.4 Thermochromism

Thermochromism is a phenomenon where a reversible change in the colour of a material occurs due to a change in the material's temperature. The material absorbs thermal energy and will reach different levels of vibrational energy depending on the absorbed amount. These vibrations result in different bonding lengths and angles, which in turn distort the geometry of the complex. This allows for the governing principles of excitation, i.e. the Laporte rule and spin selection criteria, only partly apply and hence previously forbidden transitions become allowed. The Laporte rule states that for molecules with an inversion center, orbitals which sign is unaffected by an inversion are called gerade, g . If a molecule does not have a centre of symmetry, the sign of the orbital will change during an inversion and the orbitals are denoted as ungerade, u . The Laporte rule only applies to molecules which have an inversion center, i.e. are symmetric. The spin selection criteria states that an excitation of an electron is only allowed if the spin is conserved during the excitation, and a transition must occur from g orbital to a u orbital or vice versa [24]. By cooling the complexes with liquid nitrogen to 77 K under UV-light and observing if colour is emitted or not, it is possible to deduce what deactivation pathways for the excited state that might be important.

1.6 Aim

The aim of this project is to investigate if the extent of conjugation and incorporation of nitrogen or phosphorus atoms in the ligand has an effect on the photoluminescent properties of a copper coordination complex. It shall also be determined which copper coordination complex has the most suitable photoluminescent properties for solar cell application.

2 Methods

This chapter is divided into two main sections: one describes the laboratory procedure used when creating and analyzing the complex powders, and the other describes the methods and analytical techniques used when creating the thin film solar cell.

2.1 Laboratory Method for Powder Synthesis

The general lab procedure for synthesizing all of the different complexes in powder form will be outlined. For the exact amounts of reagents used for each synthesis, read Table 1.

Table 1: Amounts of reactants used for each individual complex synthesis

Ligand	CuI [mg (mmoles)]	KI [mg (mmoles)]	Ascorbic acid [mg (mmoles)]
4,4'-bipyridine	122 (0.64)	65 (0.39)	2.29 (0.013)
Tri(o-tolyl)phosphine	63 (0.33)	35 (0.21)	1.2 (0.007)
3,6-di-2-pyridyl,1,2,4,5-tetrazine	81 (0.42)	45 (0.27)	1.5 (0.009)
Pyridine	242 (1.27)	272 (1.64)	9 (0.051)
Pyrimidine	242 (1.27)	272 (1.64)	9 (0.051)
Pyrazine	242 (1.27)	272 (1.64)	9 (0.051)
Phenanthroline	106 (0.56)	60 (0.36)	1.98 (0.010)
2,2'-bipyridine	122 (0.64)	65 (0.39)	2.29 (0.013)

The masses of CuI, KI and ascorbic acid were measured. The reactants were placed in a vial and dissolved in acetonitrile (5 mL). In another vial, the ligand (100 mg) was dissolved in acetonitrile (5 mL). Both of the solutions were left for stirring. If the ligand did not dissolve, more acetonitrile was added until it dissolved completely. Once the reactants were dissolved, the ligand solution was added to the CuI, KI and ascorbic acid solution by pipetting. When adding the ligands solution, a colour shift was immediately visible for every synthesis. After approximately fifteen minutes, the reaction was quenched with water (5 mL) and thereafter left for stirring. After 5 minutes the stirring was turned off and precipitate formed at the bottom of the vial. The supernatant was pipetted off and the precipitate was extracted into a centrifuge tube to be spinned down with acetonitrile before being washed with water. Lastly, it was washed with diethyl ether and move to another vial to be left to dry in a desiccator. For overnight storage, the vial was sealed with a lid and parafilm.

After the copper complex powders were made, several analytical measurements were made in order to determine their different characteristics. The methods were: microscopy, XRD, emission and excitation spectroscopy and time-resolved photoluminescence spectroscopy.

2.1.1 Microscopy

Microscopy was used to get an indication if the complexes were homogeneous and crystalline. If the powder had a uniform colour and repeatable shapes, it could be determined that the sample only contained product and was crystalline.

2.1.2 X-Ray Diffraction

XRD was performed with a PANalytical-X'Pert PRO diffractometer, using Cu-K α radiation. The complex in powder form was evenly distributed on the sample disc, and then inserted into the machine. The scan had a 2θ range from 4 to 80 degrees in increments of 0.008 degrees.

2.1.3 Photoluminescence Spectroscopy

Two glass plates of equal size were cut for each complex. A small amount of powder from each complex was placed with a pipette between respective glass plates and were sealed with tape. The glass plates were marked with a number for the contained complex and the procedure was repeated for all complexes. The samples were then analyzed with a flourometer and the emission and excitation wavelengths were determined.

2.1.4 Time-Resolved Photoluminescence Spectroscopy

The measurements were made on a homebuilt time-resolved photoluminescence system [25] [26]. The settings for the light source used was 100 ns between every pulse. The wavelengths used were those determined by the photoluminescence spectroscopy found in Table 4.

2.2 Laboratory Method for Thin Film Solar Cell Synthesis

After the analytical measurements were done, one complex was chosen to the thin film solar cell. The methods for preparing the substrates were identical except for the application of the copper iodide organic compound. The solar cell consisted of a glass substrate prepared with fluorine-doped tin oxide coating (FTO-coating), compact TiO₂-coating, porous TiO₂-coating, copper iodide organic complex, HTM-layer and lastly a layer of gold. The layers and their order can be seen in Figure 2. The full procedure of the preparation of the substrates apart from the the copper iodide organic layer is described in in the Sadollahkhani et al. report [14].

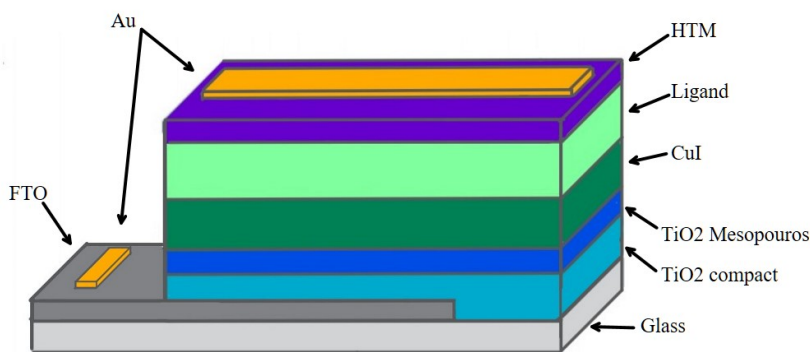


Figure 2: All layers of the copper iodide pyridine thin film solar cell.

2.2.1 Copper Iodide Organic Complex Application

The application methods for the initial copper iodide thin films on the substrates was either performed by the SILAR method or spin coating, followed by either vapour diffusion or immersion in the ligand solution. In total, ten thin film solar cells were prepared and measured in a solar simulator. To conclude what method would be the best to use for application of the copper iodide organic complex, two methods each for the copper iodide and pyridine was used and cross referenced trying all combinations of thin film synthesis. Table 2 lists the ten samples and the methods combined for making each sample.

Table 2: Array of the substrates between the methods used for thin film creation

Spin Coating		SILAR	
Vapour diffusion	Immersion	Vapour diffusion	Immersion
1	4	7	9
2	5	8	10
3	6	N/A	N/A

To prepare the cationic precursor for the SILAR method $\text{CuSO}_4 \cdot \text{H}_2\text{O}$ (0.350 g, 1.4 mmoles) was dissolved in water (14 mL). In another beaker, water (2 mL) and $\text{Na}_2\text{S}_2\text{O}_3$ (31.6 mg, 0.2 mmoles) were mixed, and then transferred to the copper(II) solution. For the anionic precursor, KI (66.5 mg, 0.4 mmoles) was dissolved in water (16 mL). The substrate was immersed in the different ionic solutions, and between each of the ionic solutions the film was rinsed with distilled water. The immersion time for each precursor is shown in the cycling scheme in Table 3 below, the cycle was repeated 30 times. When the last cycle was completed, the substrate with the formed copper iodide thin film layer was placed on a hot plate and the SILAR thin film synthesis was completed. New precursor solutions were prepared for each substrate.

Table 3: Scheme for precursor cycling in SILAR

Cationic precursor	Water	Anionic precursor	Water
5 s	3 s	20 s	3 s

The synthesis of a thin film by spin coating began by dissolving CuI (0.107 g, 5.6 mmoles) in acetonitrile (10 mL), it was left for 10 minutes to dissolve. The spinning condition was 3000 RPM, acceleration 1000 for 20 seconds. Between each layer the glass was placed on a hot plate to dry before a new layer were applied. This procedure was repeated four times for each substrate.

2.2.2 Current-Voltage Measurements

A solar simulator was used in order to measure the voltage open circuit (V_{OC}), current, efficiency and fill factor of the thin film solar cells. A certified silicon solar cell was used for calibration of the light source (collimated xenon lamp, 300W). Each thin film solar cell consisted of four miniature cells were measurements were made for one or two of these smaller cells in the middle depending on whether the V_{OC} readings were stable or not. The total illuminated area of the miniature cells which the measurements were derived from was 0.126 cm^2 .

3 Results

The results section will be divided into two different parts; one with the results collected from the synthesized powders and the other with the results collected from the thin film solar cell.

3.1 Powder Results

The synthesised complexes in powder form were observed under microscope. It was determined that all of the complex were homogeneous as only one colour could be detected for each complex. Furthermore, all of the complexes were determined to be crystalline as the complexes had a homogeneous colour and repeatable shapes. The synthesized powders were illuminated with UV-light to determine if the created complex had an emissive excited state. The registered characteristics of the complexes are summarized in Table 4. For all of the measurements except for 4,4'-bipyridine, clear results could be obtained regarding emission.

Table 4: Observed characteristics of complexes

Ligand	Observed colour	Emission under UV	Crystalline
4,4'-bipyridine	Orange-Red	N/D	Yes
Tri(o-tolyl)phosphine	White	No	Yes
3,6-di-2-pyridyl-1,2,4,5-tetrazine	Dark Grey-Brown	No	Yes
Pyridine	Off-White	Yes (Bright Yellow)	Yes
Pyrimidine	Bright Yellow	Yes (Bright Yellow)	Yes
Pyrazine	Dark Yellow	Yes (Dark Yellow)	Yes
Phenanthroline	Bright Orange	Yes (Orange)	Yes
2,2'-bipyridine	Reddish-Brown	No	Yes

3.1.1 Crystal Structures

From the XRD spectra that were obtained, five out of eight complexes had been previously reported in literature. Hence, the copper iodide organic complexes created from 4,4'-bipyridine, trio(o-tolyl)phosphine, pyridine, pyrimidine and pyrazine were concluded to be isostructural to the already reported structures when overlaying and comparing the spectra. All of the XRD spectra can be obtained in Appendix 6.1 XRD Spectra. From the photoluminescence measurements, only the complexes created from pyridine and pyrimidine gave conclusive results, therefore this section is limited to only the crystal structures for these complexes which are visible in Figure 3. For the complexes which could not be found previously in literature, these are concluded to be new crystal structures which are yet to be determined. Determining the crystal structure for the unknown complexes is outside of the scope for this project and since these complexes did not give meaningful results they are excluded from this part of the report.

Copper Iodide Pyrimidine: Space group: P 2₁/c (14). Cell: a 9.564(2) Å, b 17.689(3) Å, c 8.0729(9) Å, alpha 90, beta 108.470, gamma 90.

Copper iodide pyridine: Space group: P 21 21 21 (19). Cell: a 16.032(6) Å, b 15.510(2) Å, c 11.0756(3) Å, alpha 90, beta 90, gamma 90.

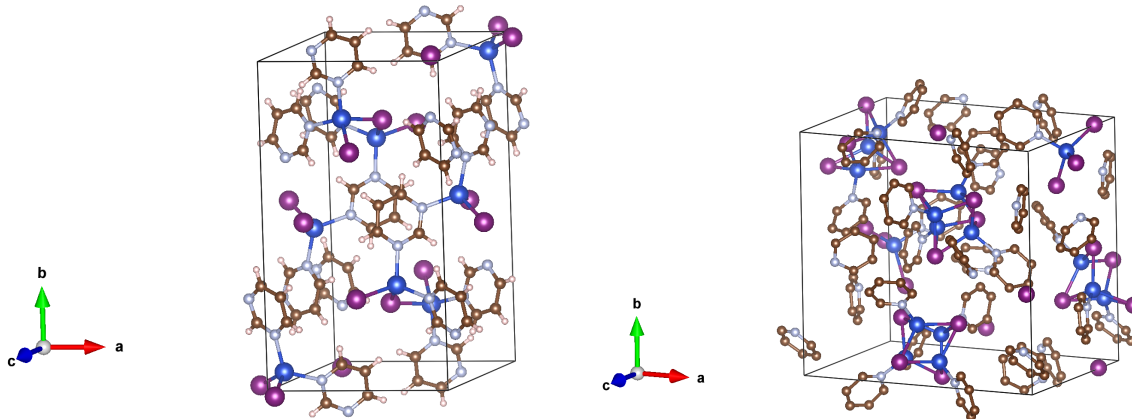


Figure 3: Simulation of crystal structures. Left: copper iodide pyrimidine. Right: copper iodide pyridine.

3.1.2 Excitation and Emission Wavelengths

Measured optimum excitation and emission wavelengths are given in Table 5. Most of the complexes did not have distinct peaks, which made the results inconclusive.

Table 5: Optimum wavelengths for emission and excitation of complexes

Ligand	Excitation [nm]	Emission [nm]
4,4'-bipyridine	N/D	N/D
Tri(o-tolyl)phosphine	N/D	N/D
3,6d-i-2-pyridyl,1,2,4,5-tetrazine	N/D	N/D
Pyridine	342	567
Pyrimidine	350	495
Pyrazine	N/D	N/D
Phenanthroline	N/D	N/D
2,2'-bipyridine	N/D	N/D

3.1.3 Time-Resolved Photoluminescence Equations

From the time-resolved photoluminescence measurements the data was fitted to a model of biexponential decay. The measurements were made for all of the eight complexes, but as only copper iodide pyridine and copper iodide pyrimidine displayed any significant properties these were the only complexes accounted for in this section. The general expression derived from equation 1.2 in the introduction that the complexes were fitted to is presented in equation 3.1.

$$y = A_1 \times e^{(t/\tau_1)} + A_2 \times e^{(t/\tau_2)} - y_0 \quad (3.1)$$

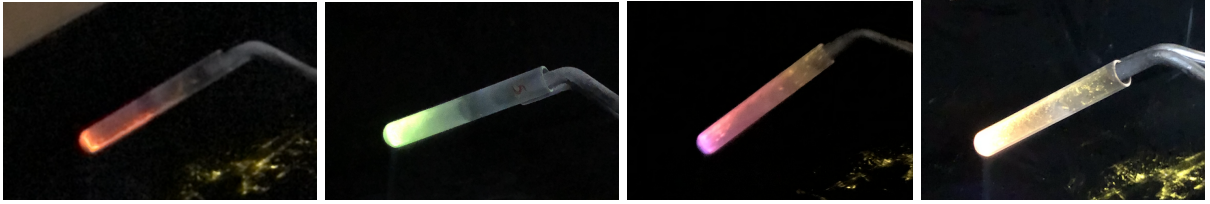
Where A_1 and A_2 are the amplitudes for the different components which gives an indication of how much each component contributes to the overall intensity of the compound. τ_1 and τ_2 are the respective lifetimes of the components and y_0 is the asymptote which the decay of the excited state approaches over time. The data fitting resulted in the parameters presented in Table 6.

Table 6: Lifetimes and amplitudes from data fitting of time-resolved photoluminescence measurements

Complex	τ_1 [s]	A_1	τ_2 [s]	A_2	y_0
Pyridine	43.2×10^{-9}	-8.7×10^{-6}	200×10^{-9}	-10^{-4}	-1.07×10^{-3}
Pyrimidine	16×10^{-9}	-4.07×10^{-4}	115×10^{-9}	-1.5×10^{-4}	-8.23×10^{-4}

3.1.4 Thermochromism

Only four of the eight copper iodide complexes showed thermochromic luminescence under UV-light when frozen with liquid nitrogen. The complexes were copper iodide tri(o-tolyl)phosphine, copper iodide pyrimidine, copper iodide pyridine, copper iodide pyrazine. The complexes with the respective emitted colours are shown in Figure 4.

**Figure 4:** Emission from copper iodide complexes frozen with liquid nitrogen in UV-light. Left to right: Copper iodide tri(o-tolyl)phosphine, copper iodide pyrimidine, copper iodide pyridine, and copper iodide pyrazine.

3.2 Solar Simulation Measurements

The solar simulator measured each individual smaller cell on the solar cell itself, which are distinguished by the four parallel golden plates. See Figure 5. The measurements were made on the ones in the middle, i.e. the second and third cell and not the first or fourth. This is due to the miniature cells in the middle being less susceptible to scratches from handling, giving a better surface to measure. In Table 7 the maximum V_{OC} , efficiency and fill factor is presented. Sample 3 was ruined in the gold evaporator due to a technical error, therefore no data was collected. Sample 6.2, 8.2 and 10.2 was not measured because the voltage was not stable. Sample 10.3 also had inconclusive results, but its J-V curve can be found in appendix 6.3. In Figure 6 the four of the best overall results from the solar simulator have been combined into a J-V-diagram which presents the current density and matching voltage for each sample cell. All the J-V-diagrams are in appendix 6.3.

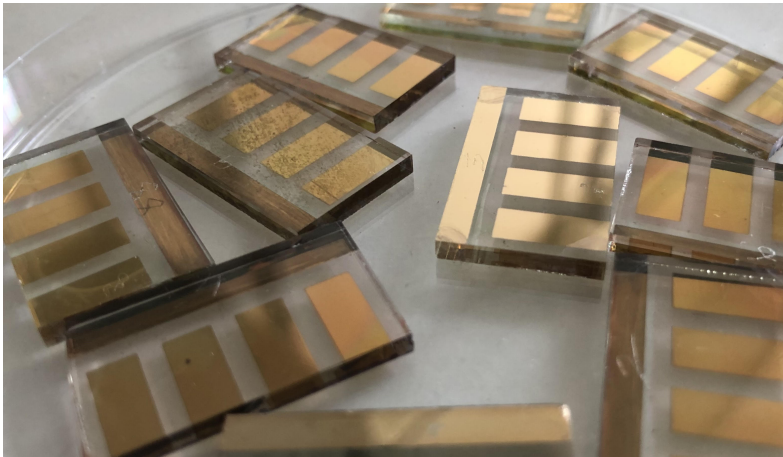
**Figure 5:** Copper iodide pyridine thin film solar cells.

Table 7: Solar cell measurements for thin film solar cells

	Miniature cell 2			Miniature cell 3		
Cell	Max V_{OC} [V]	η	Fill factor	Max V_{OC} [V]	η	Fill factor
1.	0.3	0.003	0.403	0.35	0,003	0.396
2.	N/A	N/A	N/A	0.395	0.004	0.369
3.	N/A	N/A	N/A	N/A	N/A	N/A
4.	0.37	0.004	0.379	0.365	0.003	0.342
5.	0.38	0.005	0.384	0.38	0.005	0.425
6.	N/A	N/A	N/A	0.40	0.005	0.397
7.	0.355	0.002	0.366	0.355	0.003	0.358
8.	N/A	N/A	N/A	0.275	0.002	0.427
9.	0.295	0.002	0.374	0.295	0.002	0.352
10.	N/A	N/A	N/A	N/A	N/A	N/A

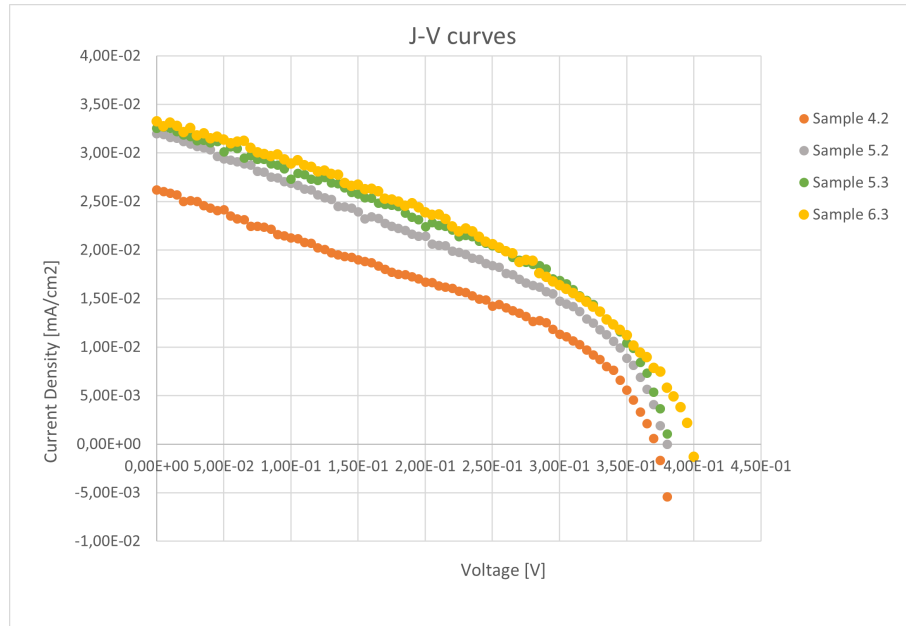


Figure 6: J-V curves from the sample cells with the best result.

To summarize, the overall solar cells with the highest and thus best measurements were the ones made using spin coating and immersion. Looking at the data from Table 7 and the graphs of the J-V curves in appendix 6.3, sample 5.3 is the overall most promising solar cell.

4 Discussion

The measurements from the time-resolved photoluminescence analysis proved that most of the complexes did not show any significant photoluminescent properties. This was hinted beforehand, as most of the complexes when examined under UV-light showed no, or only what was deemed to be a faint, emission of colour apart from the complexes created with the pyridine and the pyrimidine ligands which gave bright emission. As stated earlier in the introduction, this could be due to not excluding oxygen hence oxidization might have occurred. Later, in the time-resolved photoluminescence measurements, these complexes were also the only ones that gave sufficient results. For both the complexes, the determined half-lives for the short-lived excited state compared to the long-lived excited state presented in Table 6 was smaller by a magnitude of 10^{-1} . Comparing the curves in Appendix 6.2, the copper iodide pyrimidine complex displays a more fitting curve for a material which is supposed to be used in a solar cell, as it has a rapidly decaying short-lived excited state. Also, comparing the equations presented in Table 6 that were produced for the fitting of the data from the time-resolved photoluminescence measurements, the copper iodide pyrimidine complex had a significantly shorter half-life for the excited state. As stated in the introduction, a shorter half-life suggests that there are quenching processes taking place and hopefully the process taking place is the creation of electron-hole pairs. Therefore, if the thin film solar cells were made of the complexes from pyrimidine instead of pyridine there is a possibility to have recorded better performance of the solar cells from the solar simulator measurements. Due to the restricted amount of available pyrimidine ligand, it was not made in to a solar cell. As the pyridine complex was the only other complex which gave sufficient results, this became the choice for the thin film solar cell.

The photoluminescence measurements only gave conclusive results for complexes created from pyridine and pyrimidine and one could argue that the smaller ligands tended to give the complexes better photoluminescent properties. However, this result is contradictory to the findings from earlier reports presented in the introduction, which have reported that larger conjugated systems in dye sensitized solar cells leads to better power conversion efficiency. One theory for smaller ligands being more suiting is that smaller complexes can tightly pack together and arrange in a repeating pattern. Bigger, bulkier ligands may not pack together as closely as they take up more space and are also able to rotate around sigma bonds, hence their arrangement may not be as crystalline. As only few different ligands have been investigated in this study and most of the results were inconclusive when it comes to the level of conjugation and number of nitrogen or phosphorus atoms, there is a possibility that there are other aspects that affect the complexes. For example, the complexes have earlier been stated to be reactive with oxygen. The syntheses were not carried out under inert conditions so there is a high probability that the complexes have oxidized. To confirm this, the analytical measurement should have been run directly after the syntheses, and then periodically to obtain a complete picture of whether the complexes had photoluminescent properties and if they are oxidized. These results however may prove that the complexes created with pyridine and pyrimidine are more stable in an open environment.

The copper iodide complexes that did show a colour change, presented in Table 4, when cooled with liquid nitrogen and exposed to UV-light were tri(o-tolyl)phosphine, pyrimidine, pyridine and pyrazine. This indicates that the created thin film solar cells may not be the ultimate use for these types of copper halide organic complexes. However, the complexes which only displayed photoluminescence when cooled with liquid nitrogen and not at room temperature suggests that vibrational relaxation is an important excited-state deactivation pathway and may prove to be useful in other applications such as temperature sensory devices or catalysis.

As for the choice of pyridine as the ligand for the solar cell, there are definitely better choices of ligand in terms of sustainability. Pyridine is a flammable liquid which causes acute toxicity both orally and when in contact with skin. As for the second choice of ligand which would have been pyrimidine, it is

also flammable. An aspect which might speak for the use of pyrimidine derivatives is that substituted pyrimidines such as uracil and cytosine, visible in Figure 7, are crucial building blocks in genomes. Some substituted pyrimidines are abundant in nature, which could imply that if these give copper halide organic complexes photoluminescent properties suited for photovoltaic process, then substituted pyrimidines can be a less dangerous choice. For example, if cytosine would accidentally be released into the environment there are natural processes which can degrade it. To examine in future studies if pyrimidine or substituted pyrimidines could result in copper halide organic solar cells with adequate efficiency would also be in accordance with green chemistry methods.

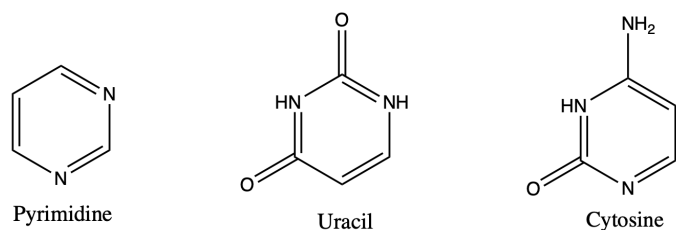


Figure 7: Structures of pyrimidine, uracil, and cytosine.

During the SILAR method, some of the substrates were either dropped in the precursor solutions or scratched by the tweezers that were used to hold the substrates, which means that the layers of copper iodide were not completely uniform. In addition to this, it was visible that the layers formed on the substrate surface varied in transparency. This would result in an uneven surface when the ligand was applied with both vapour diffusion and immersion. This could explain that the overall results from the solar cells presented in Table 7 were better for spin coating followed by immersion. This could be due to the spin coating giving a more even distribution of the material, and in accordance with the Bloch's theorem briefly discussed in the introduction could lead to the single electron wave functions being able to combine more sufficiently throughout the material than when made by SILAR method.

When comparing the results from the solar simulator both in Table 7, the maximum V_{OC} and efficiency were lower overall for the thin film solar cells created with the SILAR method compared to the thin film solar cells created with spin coating. In addition, three of the miniature cells from the thin films created with SILAR were not stable when conducting the experiments, meaning that the readings jumped between different values of maximum V_{OC} . In general, the solar cells created by spin coating gave overall better results in the solar simulator than the ones created by the SILAR method. The reason for the low V_{OC} and fill factor might be due the method used to prepare the substrate coatings for the thin film solar cell. Since the method from Sadollahkhani et al. is refined for another type of electron donor, the coatings would have to be changed in order to be perfected of this particular copper iodide organic complex. Improvements could be a protective layer providing a barrier between the complex and oxygen or changes to the HTM-layer.

As already mentioned, the best method for creating the thin film solar cell was spin coating followed by immersion in the ligand solution. However, immersion might not be the best method from a perspective of green chemistry methods. Immersion demands a lot of ligand in order to be applied, compared to vapour diffusion for example. Saving resources and material is always worth striving towards for a sustainable future. This is not central for the making of the solar cell at this early stage in the process, but it is a major part of the green chemistry principles that should always be considered.

5 Conclusion

The copper iodide complexes created from pyridine and pyrimidine were the only complexes that gave conclusive measurements in the time-resolved photoluminescence measurements, which is contradictory to what might have been expected from smaller ligands from previous studies. For a more comprehensive study, more ligands with different extent of conjugation and number of nitrogen or phosphorus atoms could have been used. The thin film solar cell created with the copper iodide pyridine complex gave overall low readings independently of what methods were used to create the thin films. The best overall obtained readings were recorded from sample 5.3; 0.38 V, 0.005 efficiency and 0.425 fill factor. Sample 5.3 was made using spin coating for applying copper iodide and immersion for the ligand. For future studies, it may be worthwhile to make the solar cell with the copper iodide pyrimidine complex which gave the best time-resolved photoluminescence results.

Bibliography

- [1] W. Bank. (2020). “Lighting up africa: Bringing renewable, off-grid energy to communities”, [Online]. Available: <https://www.worldbank.org/en/news/feature/2020/08/13/lighting-up-africa-bringing-renewable-off-grid-energy-to-communities> (visited on 03/29/2021).
- [2] IEA. (2020). “Renewables 2020”, [Online]. Available: <https://www.iea.org/reports/renewables-2020> (visited on 03/29/2021).
- [3] C. Endeavour, *Chemical Sciences*. 2019, pp. 214–222. [Online]. Available: <https://careerendeavour.in/wp-content/uploads/2018/09/coordination-chemistry.pdf>.
- [4] R. Peng, M. Li, and D. Li, “Copper(i) halides: A versatile family in coordination chemistry and crystal engineering”, *Coordination Chemistry Reviews*, vol. 254, no. 1, pp. 1–18, 2010, ISSN: 0010-8545. DOI: <https://doi.org/10.1016/j.ccr.2009.10.003>. [Online]. Available: <https://www.sciencedirect.com/science/article/pii/S0010854509002653>.
- [5] M. K. Nazeeruddin, A. Kay, I. Rodicio, R. Humphry-Baker, E. Mueller, P. Liska, N. Vlachopoulos, and M. Graetzel, “Conversion of light to electricity by cis-x2bis(2,2'-bipyridyl-4,4'-dicarboxylate)ruthenium(ii) charge-transfer sensitizers (x = cl-, br-, i-, cn-, and scn-) on nanocrystalline titanium dioxide electrodes”, *Journal of the American Chemical Society*, vol. 115, no. 14, p. 6385, 1993. DOI: 10.1021/ja00067a063. [Online]. Available: <https://doi.org/10.1021/ja00067a063>.
- [6] L. S. Xie, G. Skorupskii, and M. Dincă, “Electrically conductive metal–organic frameworks”, *Chemical Reviews*, vol. 120, no. 16, pp. 8536–8580, 2020, PMID: 32275412. DOI: 10.1021/acs.chemrev.9b00766. eprint: <https://doi.org/10.1021/acs.chemrev.9b00766>. [Online]. Available: <https://doi.org/10.1021/acs.chemrev.9b00766>.
- [7] M. Cariello, S. Ahn, K.-W. Park, S.-K. Chang, J. Hong, and G. Cooke, “An investigation of the role increasing -conjugation has on the efficiency of dye-sensitized solar cells fabricated from ferrocene-based dyes”, *RSC Adv.*, vol. 6, pp. 9132–9138, 11 2016. DOI: 10.1039/C5RA21565J. [Online]. Available: <http://dx.doi.org/10.1039/C5RA21565J>.
- [8] L.-W. Ma, Z.-S. Huang, S. Wang, H. Meier, and D. Cao, “Impact of -conjugation configurations on the photovoltaic performance of the quinoxaline-based organic dyes”, *Dyes and Pigments*, vol. 145, pp. 126–135, 2017, ISSN: 0143-7208. DOI: <https://doi.org/10.1016/j.dyepig.2017.05.054>. [Online]. Available: <https://www.sciencedirect.com/science/article/pii/S0143720817303807>.
- [9] C. E. Housecroft and E. C. Constable, “The emergence of copper(i)-based dye sensitized solar cells”, *Chem. Soc. Rev.*, vol. 44, pp. 8386–8398, 23 2015. DOI: 10.1039/C5CS00215J. [Online]. Available: <http://dx.doi.org/10.1039/C5CS00215J>.
- [10] C. Kittel, *Introduction to solid state physics*. John Wiley & Sons, 1953.
- [11] S. E. Hassan H Griffin J, “Spin coating: Complete guide to theory and technique”, [Online]. Available: <https://www.ossila.com/pages/spin-coating>.
- [12] L. C. Pathan H.M, “Deposition of metal chalcogenide thin films by successive ionic layer adsorption and reaction (silar) method”, *Bullentin of Materials Science*, vol. 27, no. 2, pp. 85–111, 2004. [Online]. Available: <https://link.springer.com/content/pdf/10.1007/BF02708491.pdf>.
- [13] B. C. (2020). “Chemistry in pictures: Vapor diffusion”, [Online]. Available: <https://cen.acs.org/synthesis/Chemistry-Pictures-Vapor-diffusion/98/web/2020/02>.
- [14] A. Sadollahkhani, P. Liu, V. Leandri, M. Safdari, W. Zhang, and J. Gardner, “Energetic barriers to interfacial charge transfer and ion movement in perovskite solar cells”, *ChemPhysChem*, vol. 18, pp. 3047–3055, Aug. 2017. DOI: 10.1002/cphc.201700740.

- [15] S. N. Habisreutinger, D. P. McMeekin, H. J. Snaith, and R. J. Nicholas, "Research update: Strategies for improving the stability of perovskite solar cells", *APL Materials*, vol. 4, no. 9, pp. 3–5, 2016. DOI: 10.1063/1.4961210. eprint: <https://doi.org/10.1063/1.4961210>. [Online]. Available: <https://doi.org/10.1063/1.4961210>.
- [16] K. M. Rajiv Kohli, *Developments in Surface Contamination and Cleaning, Volume 12*. Elsevier, 2019.
- [17] A. Rajeswari, E. J. S. Christy, E. S. Gopi, K. Jayaraj, and A. Pius. (2020). "Characterization studies of polymer-based composites related to functionalized filler-matrix interface", [Online]. Available: <https://www.sciencedirect.com/science/article/pii/B9780081026656000091> (visited on 04/12/2021).
- [18] F. L. D. Adnan Mujahid. (20212). "Chapter 6 - molecularly imprinted polymers for sensors: Comparison of optical and mass-sensitive detection", [Online]. Available: <https://www.sciencedirect.com/science/article/pii/B9780444563316000062#s0030> (visited on 04/12/2021).
- [19] M. W. D. Mortimer Abramowitz. (2020). "Flourescence - overview of fluorescence excitation and emission fundamentals", [Online]. Available: <https://www.olympus-lifescience.com/en/microscope-resource/primer/lightandcolor/fluoroexcitation/>.
- [20] Anon. (2019). "Photoluminescence spectroscopy", [Online]. Available: https://chem.libretexts.org/Courses/Northeastern_University/10%3A_Spectroscopic_Methods/10.6%3A_Photoluminescence_Spectroscopy (visited on 04/12/2021).
- [21] J. R. Lakowicz, *Principles of Flourescence Spectroscopy*. Springer, 2010.
- [22] U. Bhattacharjee, "Application of spectroscopy and super-resolution microscopy: Excited state", DOI: 10.2172/1342545. [Online]. Available: <https://www.osti.gov/biblio/1342545>.
- [23] M. Abrahamsson, "Tuning of the excited state properties of ruthenium(ii)- polypyridyl complexes.", 2006. [Online]. Available: <http://www.diva-portal.org/smash/get/diva2:169167/FULLTEXT01.pdf>.
- [24] M. J. Winters, *D-block Chemistry*. Oxford University Press, 2015.
- [25] V. Leandri, P. Liu, A. Sadollahkhani, M. Safdari, L. Kloo, and J. M. Gardner, "Excited-state dynamics of [ru(bpy)3]2+ thin films on sensitized tio2 and zro2", *ChemPhysChem*, vol. 20, no. 4, pp. 618–626, 2019. DOI: <https://doi.org/10.1002/cphc.201801010>. eprint: <https://chemistry-europe.onlinelibrary.wiley.com/doi/pdf/10.1002/cphc.201801010>. [Online]. Available: <https://chemistry-europe.onlinelibrary.wiley.com/doi/abs/10.1002/cphc.201801010>.
- [26] L. Wang, F. Zhang, T. Liu, W. Zhang, Y. Li, B. Cai, L. He, Y. Guo, X. Yang, B. Xu, J. M. Gardner, L. Kloo, and L. Sun, "A crosslinked polymer as dopant-free hole-transport material for efficient n-i-p type perovskite solar cells", *Journal of Energy Chemistry*, vol. 55, pp. 211–218, 2021, ISSN: 2095-4956. DOI: <https://doi.org/10.1016/j.jechem.2020.06.062>. [Online]. Available: <https://www.sciencedirect.com/science/article/pii/S2095495620304794>.

6 Appendix

In the following sections, complementary data which has not been featured explicitly in the report from the laborative work will be inserted as appendices.

6.1 X-Ray Diffraction Spectra

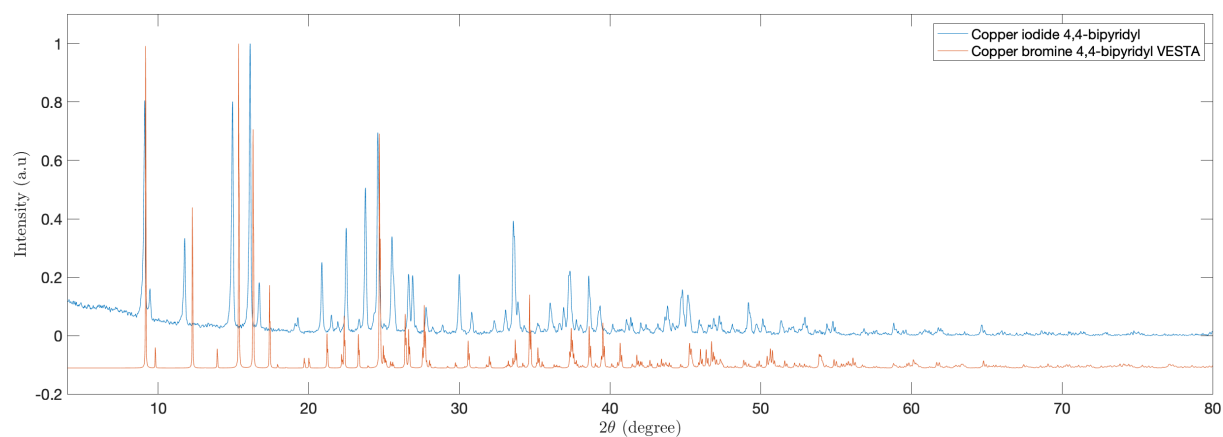


Figure 8: Overlay of XRD of copper iodide 4,4-bipyridyl complex from measurement and simulated Copper bromide 4,4-bipyridyl XRD pattern.

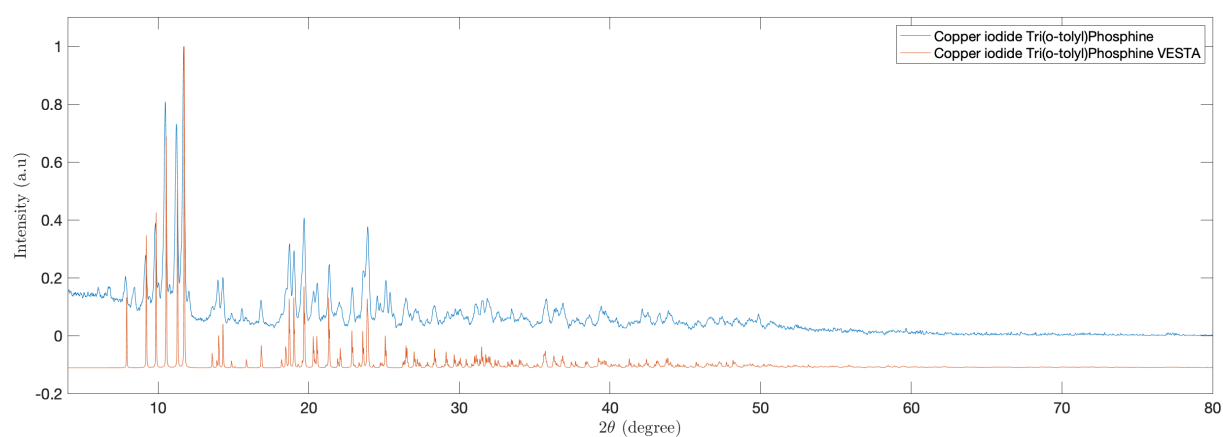


Figure 9: Overlay of XRD of copper iodide trio(o-tolyl)phosphine complex from measurement and simulated XRD pattern.

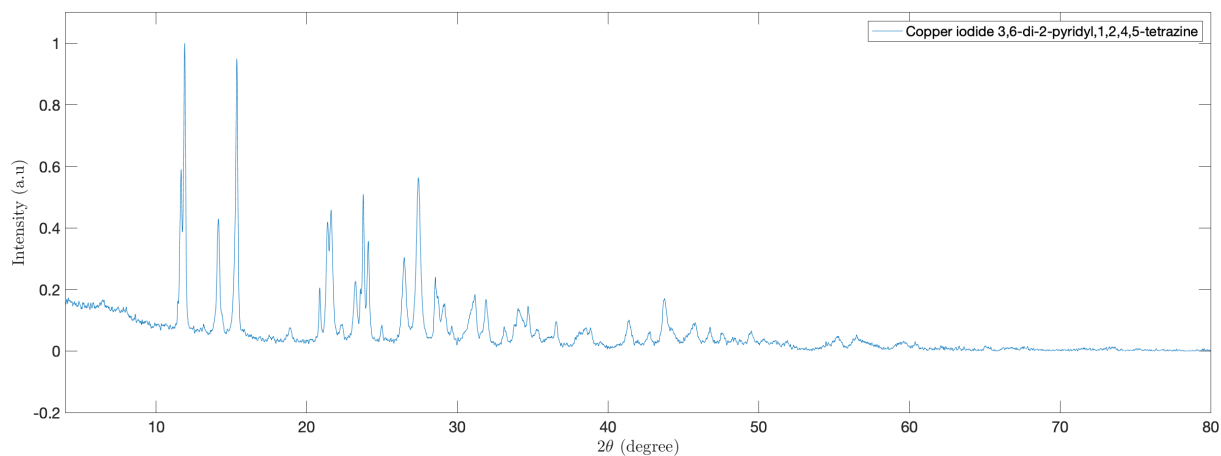


Figure 10: XRD pattern from copper iodide 3,6-di-2-pyridyl,1,2,4,5-tetrazine complex.

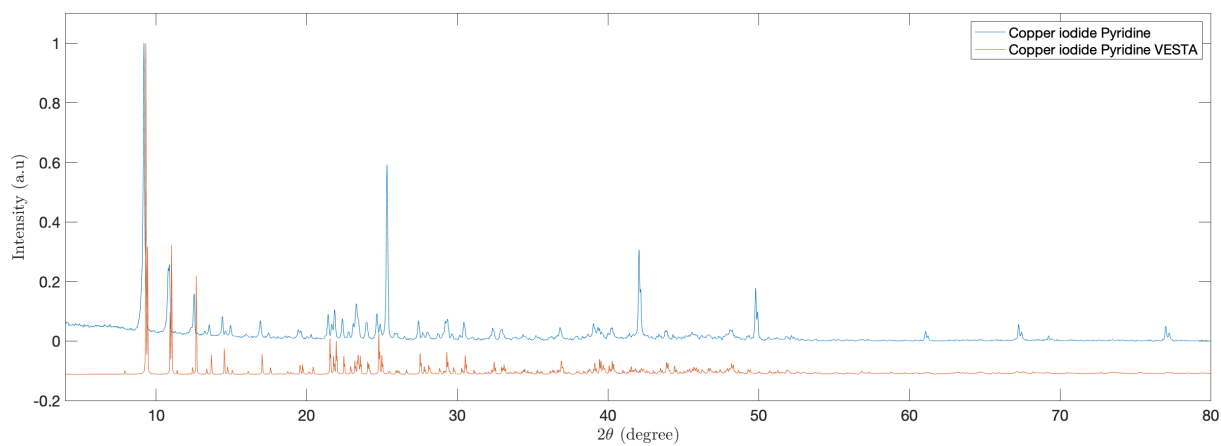


Figure 11: Overlay of XRD of copper iodide pyridine complex from measurement and simulated XRD pattern.

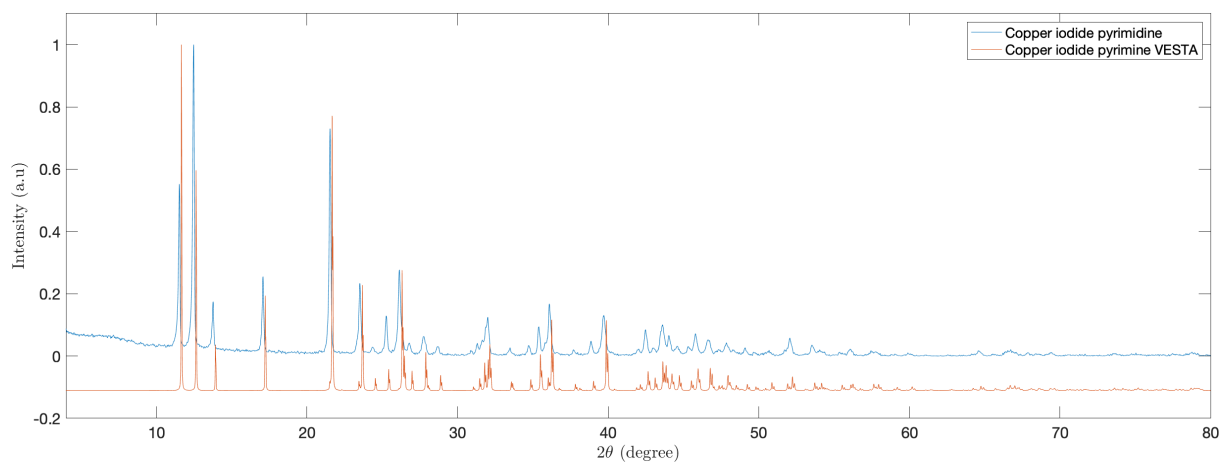


Figure 12: Overlay of XRD of copper iodide pyrimidine complex from measurement and simulated XRD pattern.

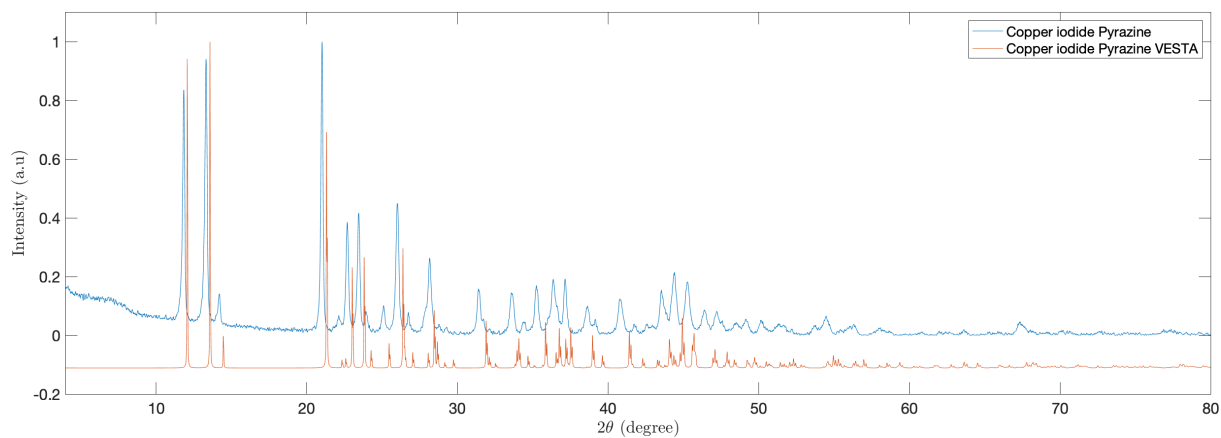


Figure 13: Overlay of XRD of copper iodide pyrazine complex from measurement and simulated XRD pattern.

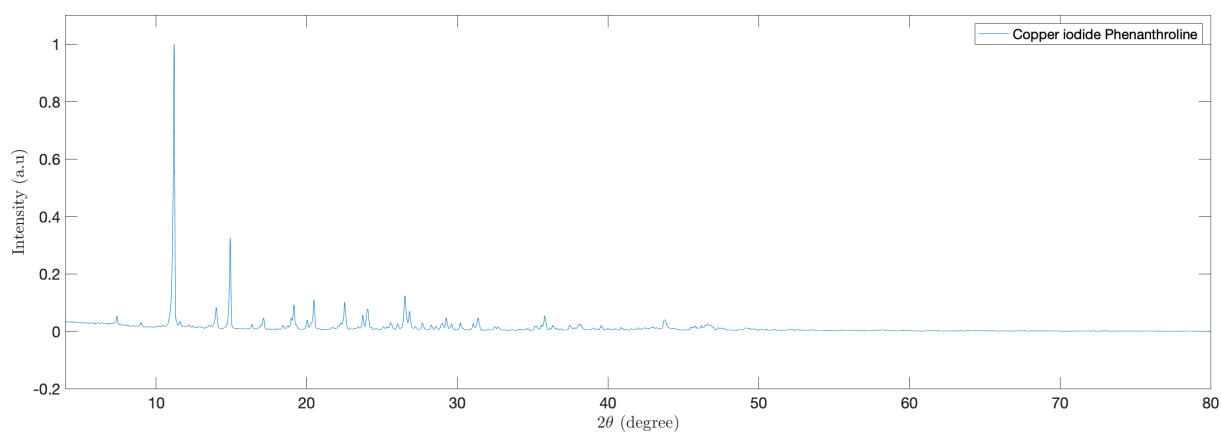


Figure 14: XRD pattern from copper iodide phenanthroline complex.

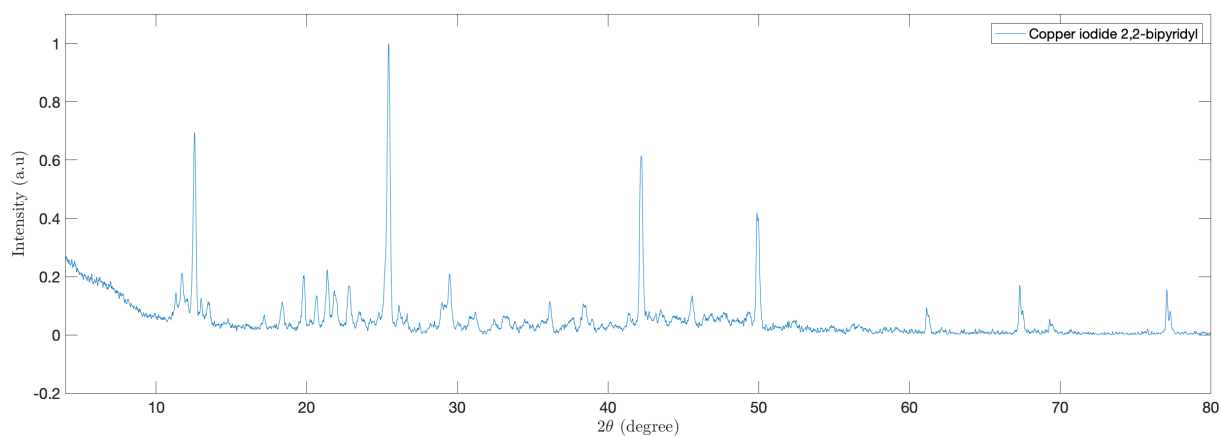


Figure 15: XRD pattern from copper iodide 2,2'-bipyridyl complex.

6.2 Time-Resolved Photoluminescence Data

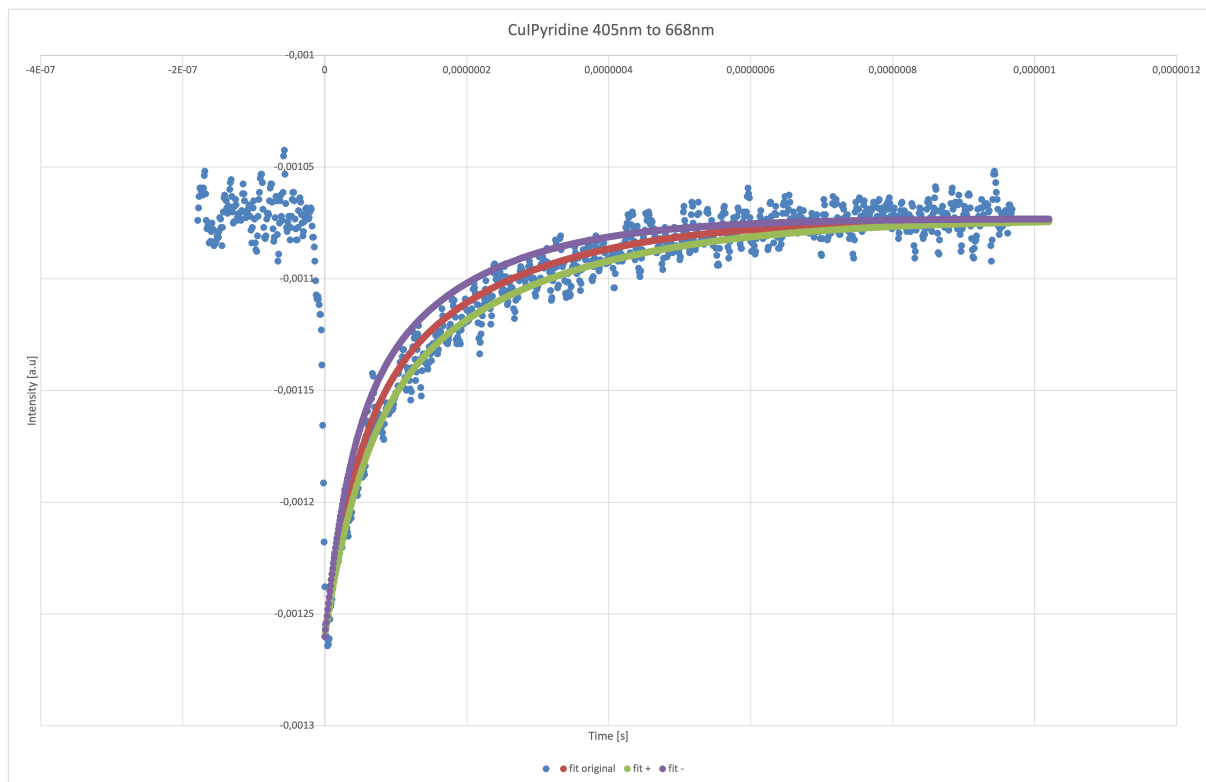


Figure 16: Fitted data for copper iodide pyridine complex in powder from TRPL measurements.

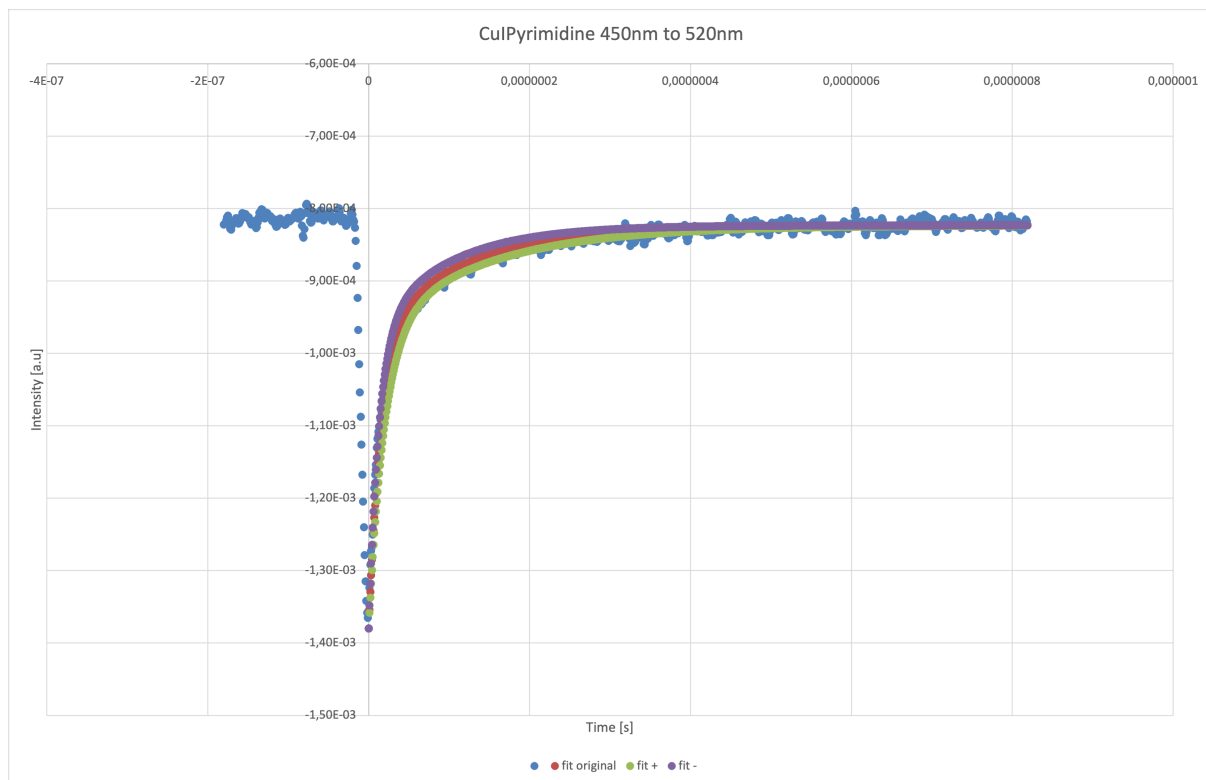


Figure 17: Fitted data for copper iodide pyrimidine complex in powder from TRPL measurements.

6.3 J-V curves from Solar Simulator

In the following section, the J-V curves from the solar simulator are displayed.

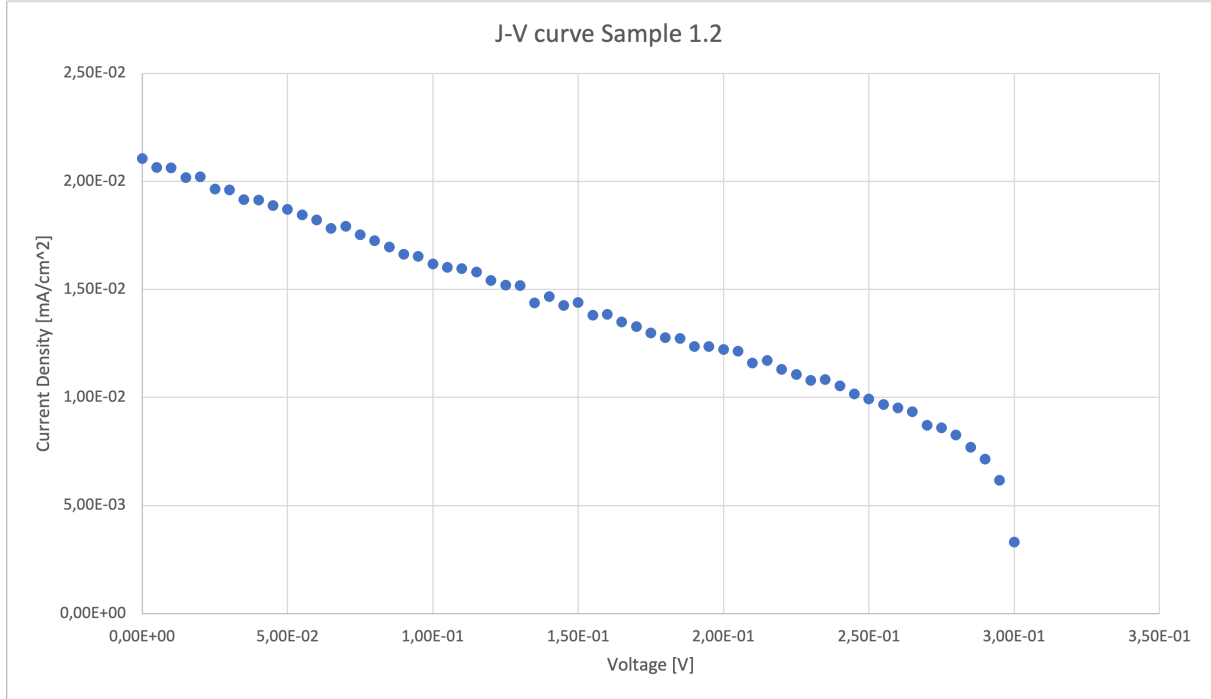


Figure 18: J-V curve from miniature cell 1.2.

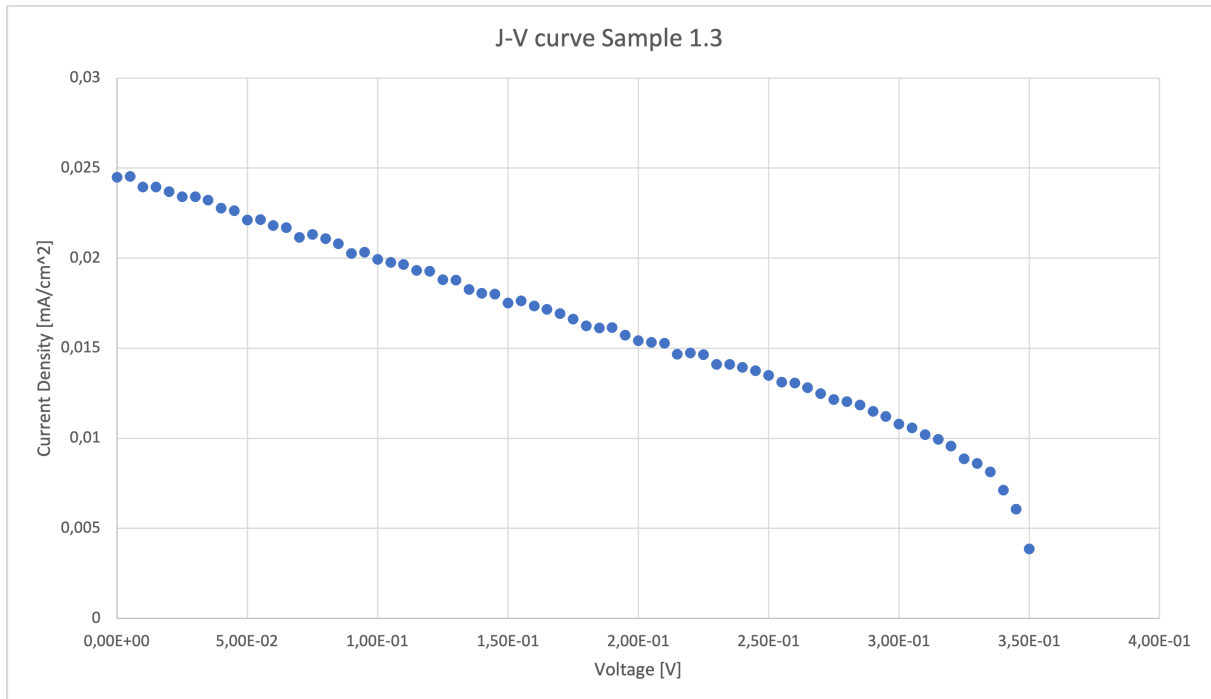


Figure 19: J-V curve from miniature cell 1.3.

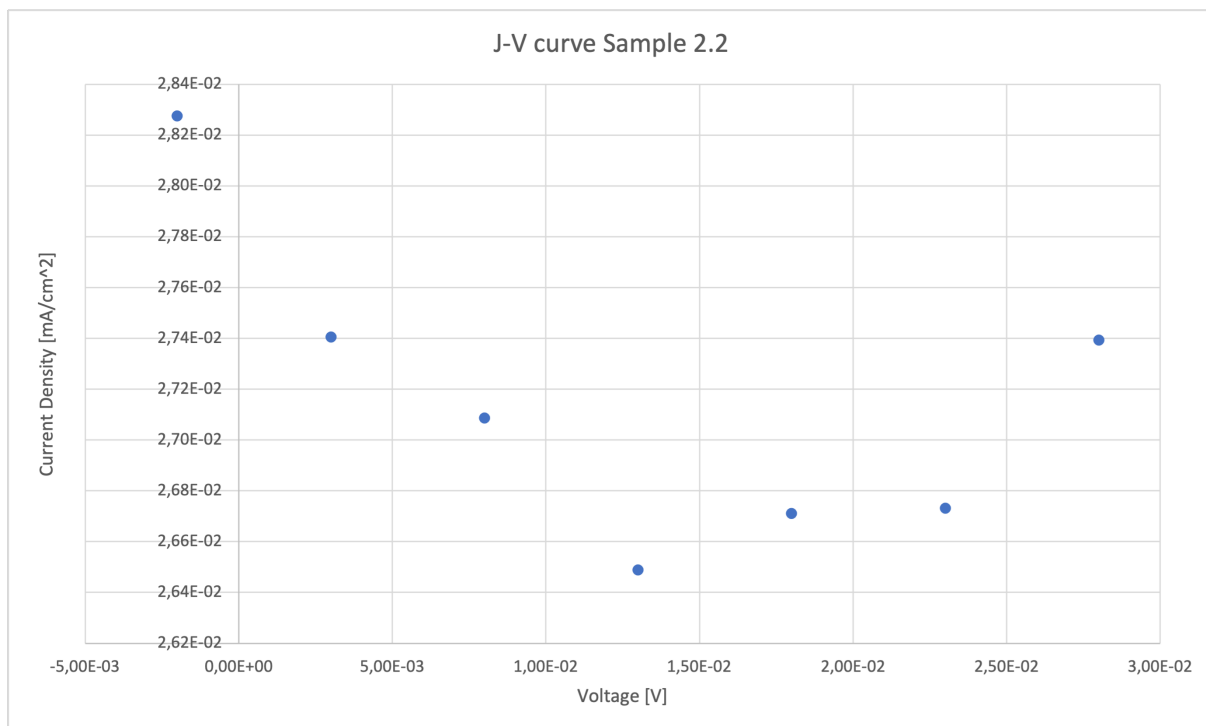


Figure 20: J-V curve from miniature cell 2.2.

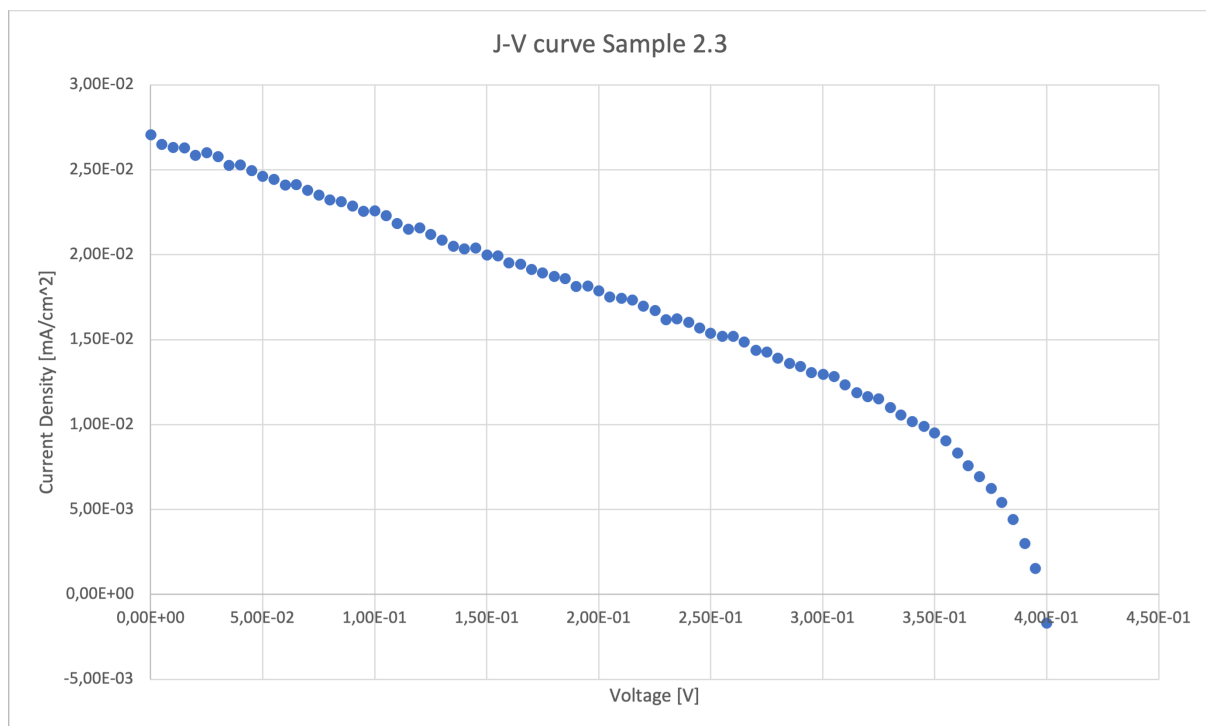


Figure 21: J-V curve from miniature cell 2.3.

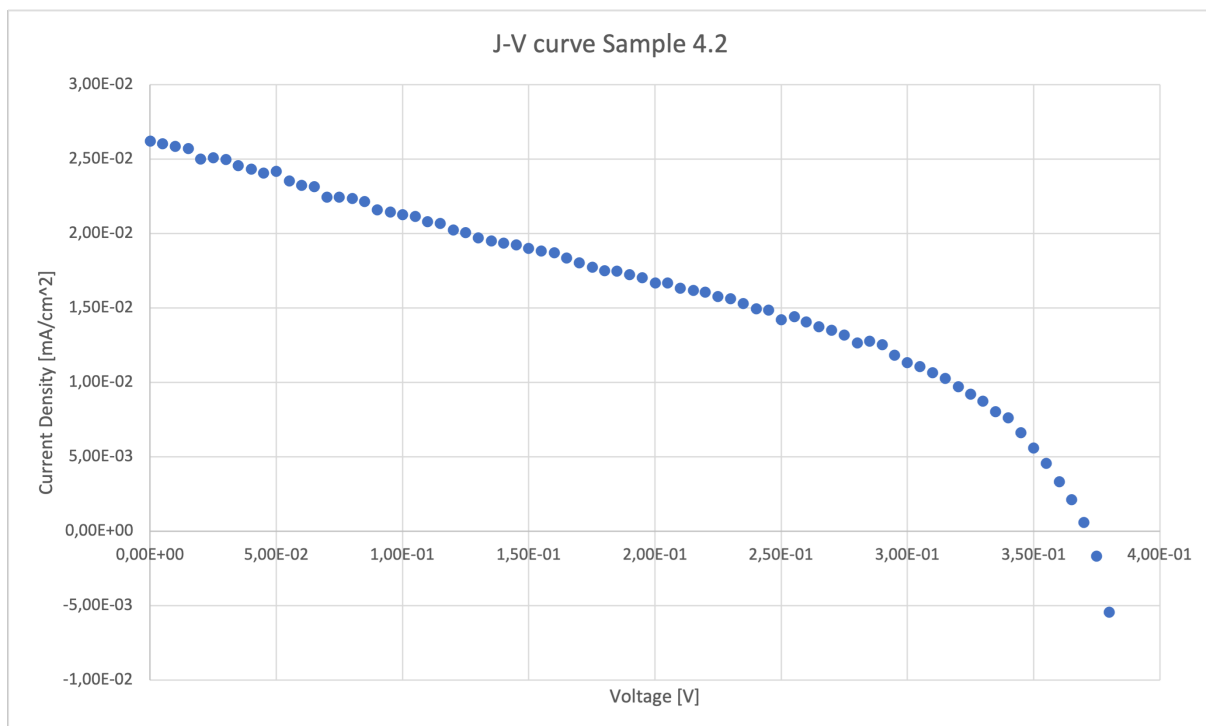


Figure 22: J-V curve from miniature cell 4.2.

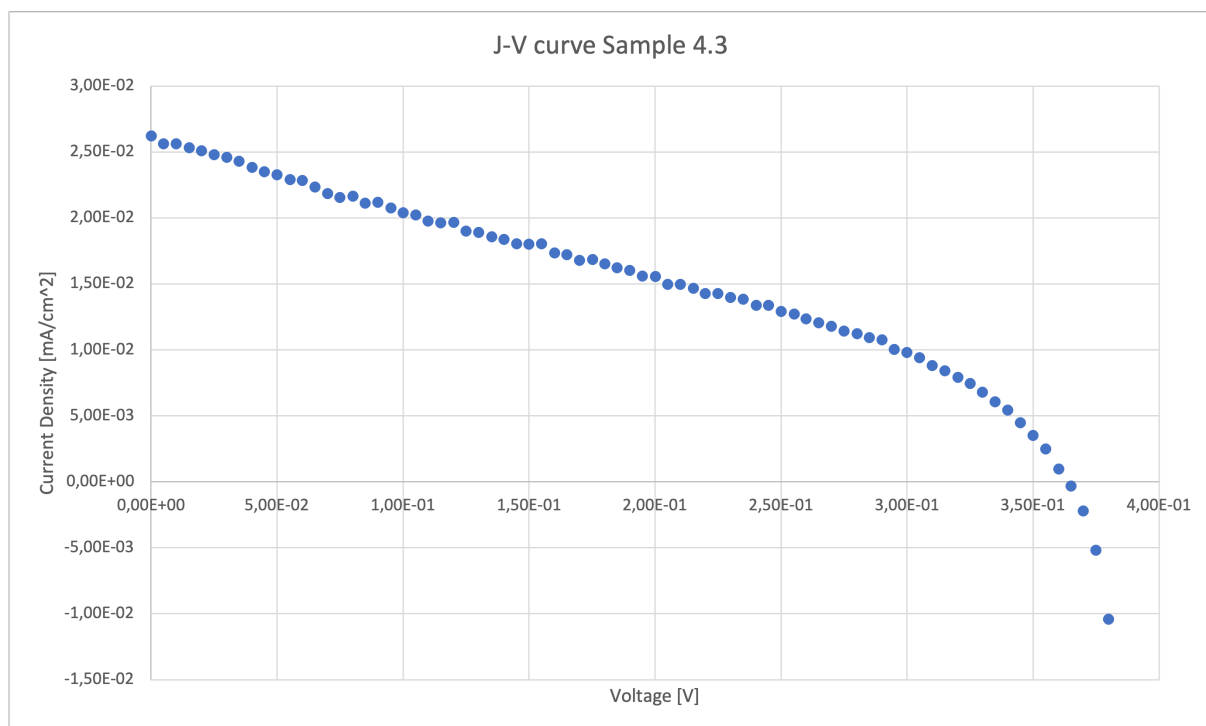


Figure 23: J-V curve from miniature cell 4.3.

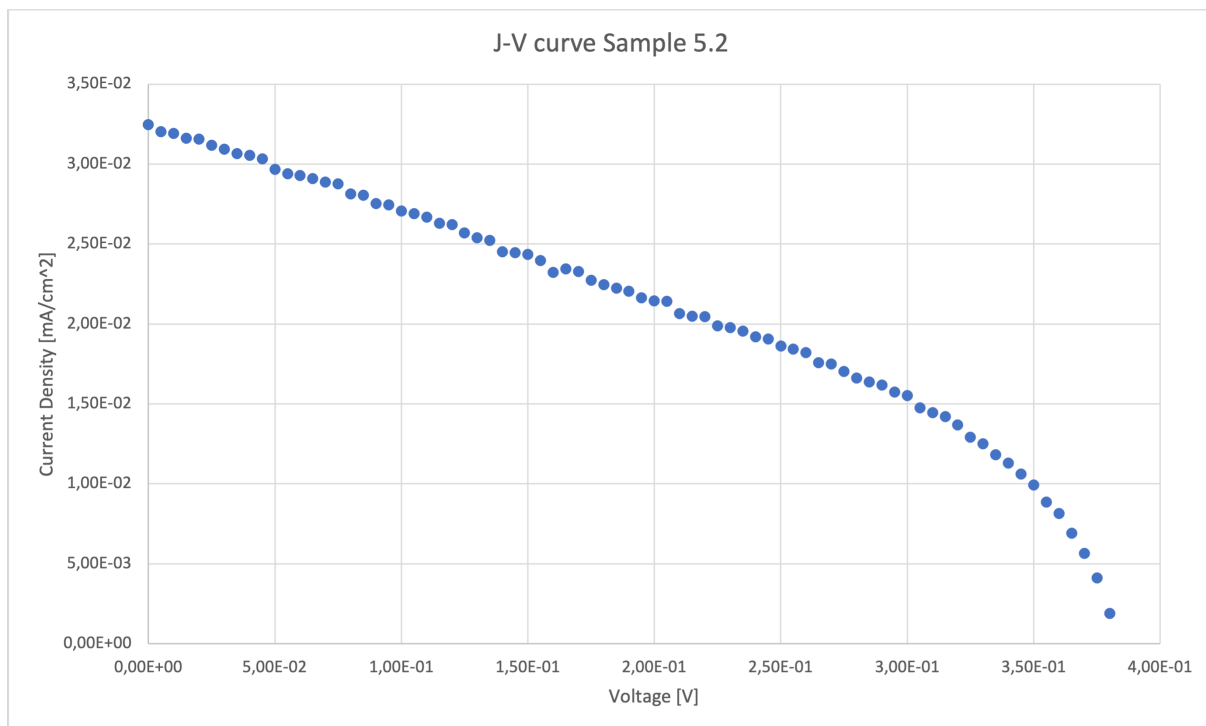


Figure 24: J-V curve from miniature cell 5.2.

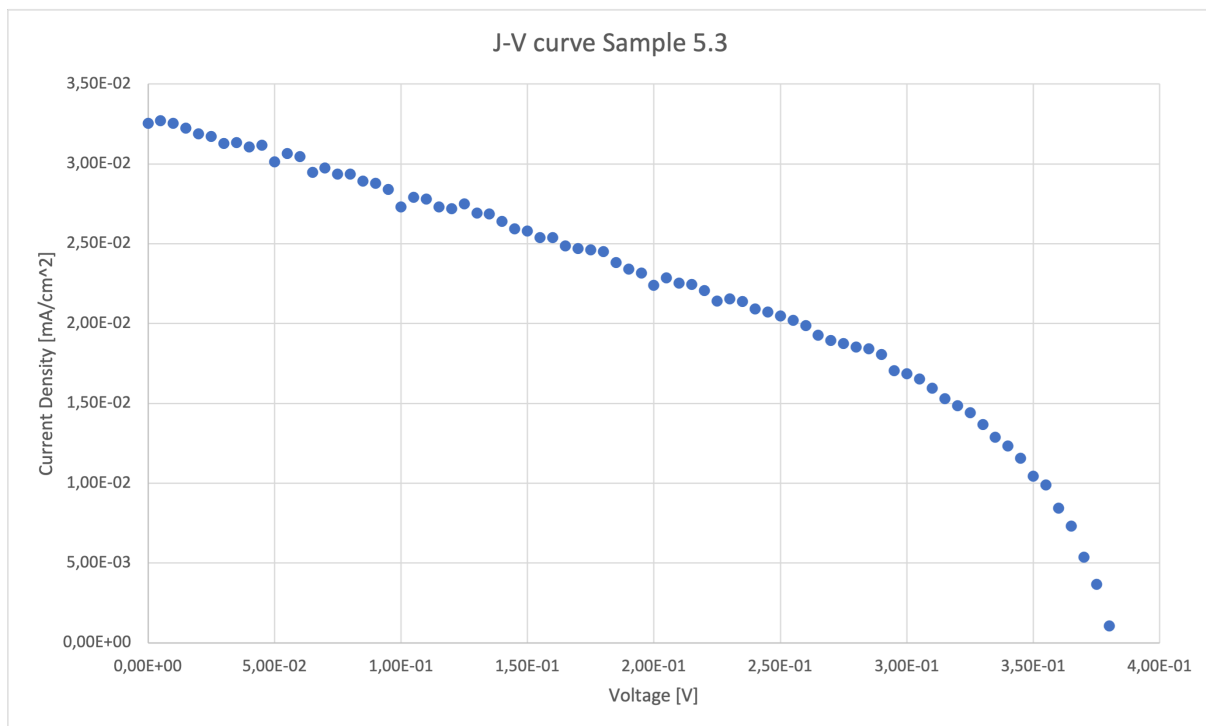


Figure 25: J-V curve from miniature cell 5.3.

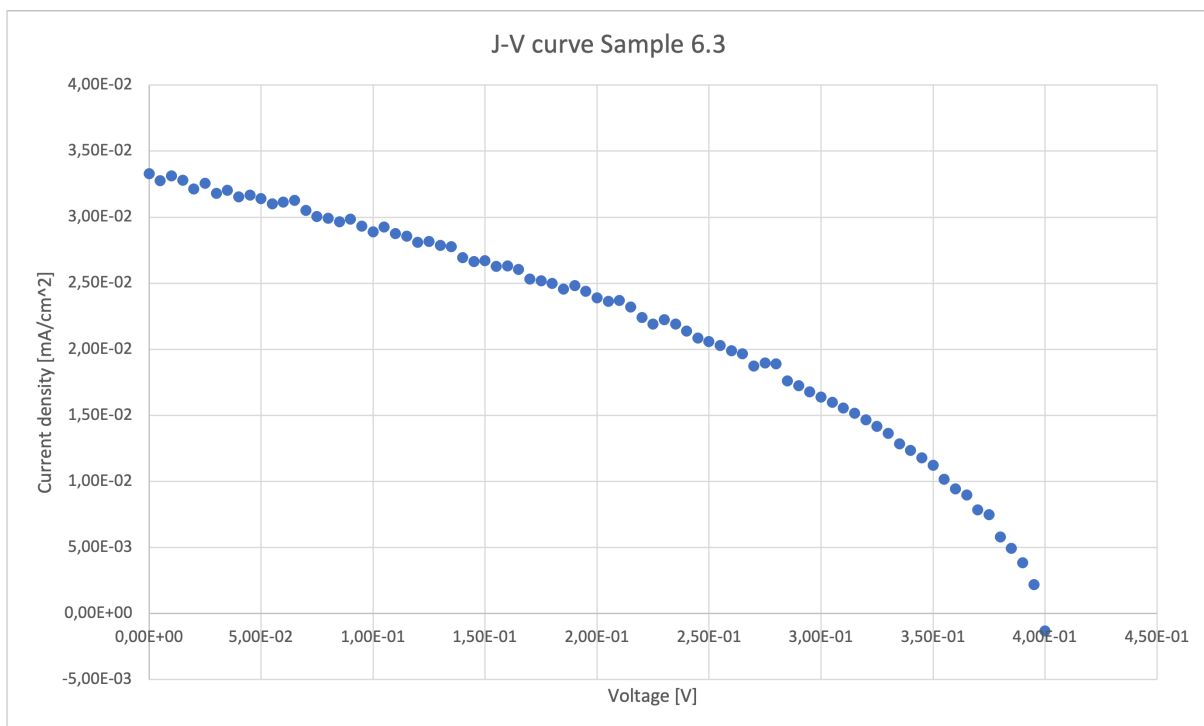


Figure 26: J-V curve from miniature cell 6.3.

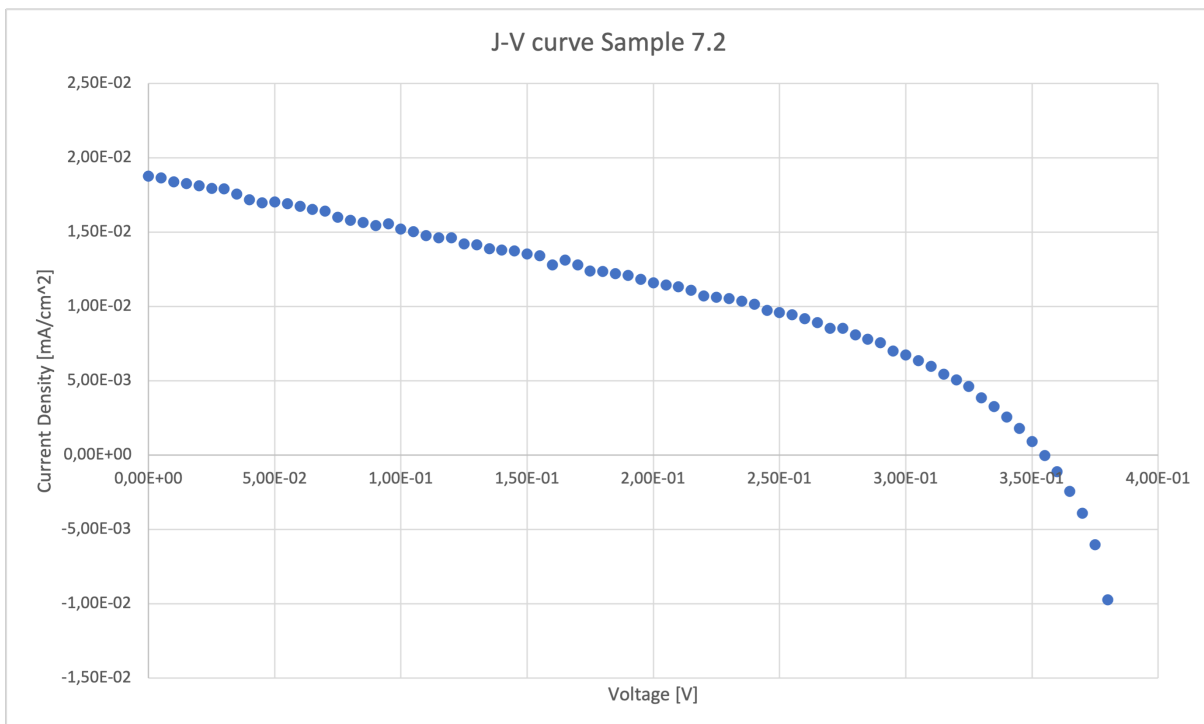


Figure 27: J-V curve from miniature cell 7.2.

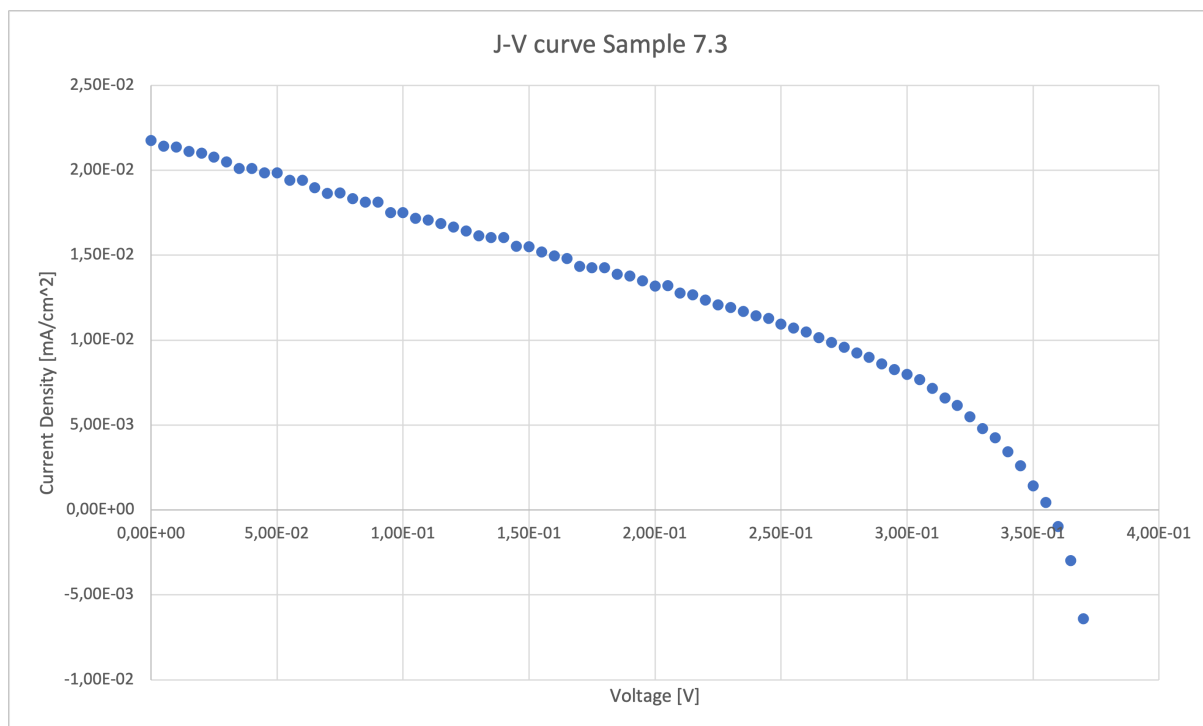


Figure 28: J-V curve from miniature cell 7.3.

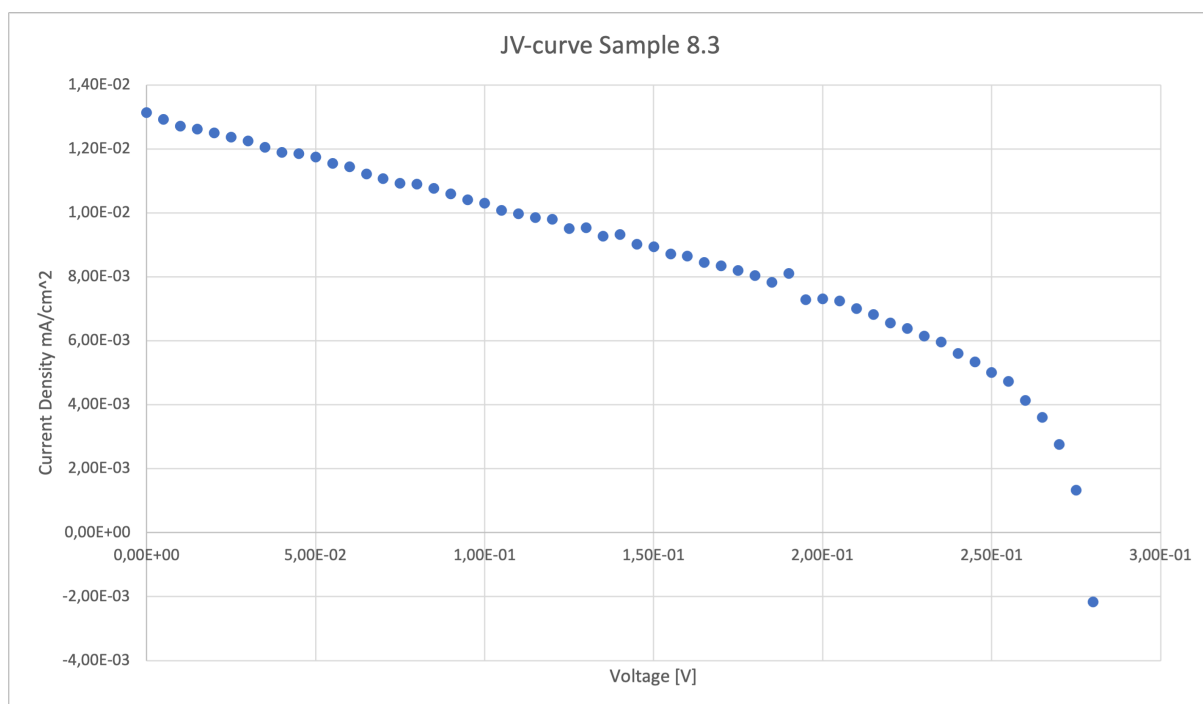


Figure 29: J-V curve from miniature cell 8.3.

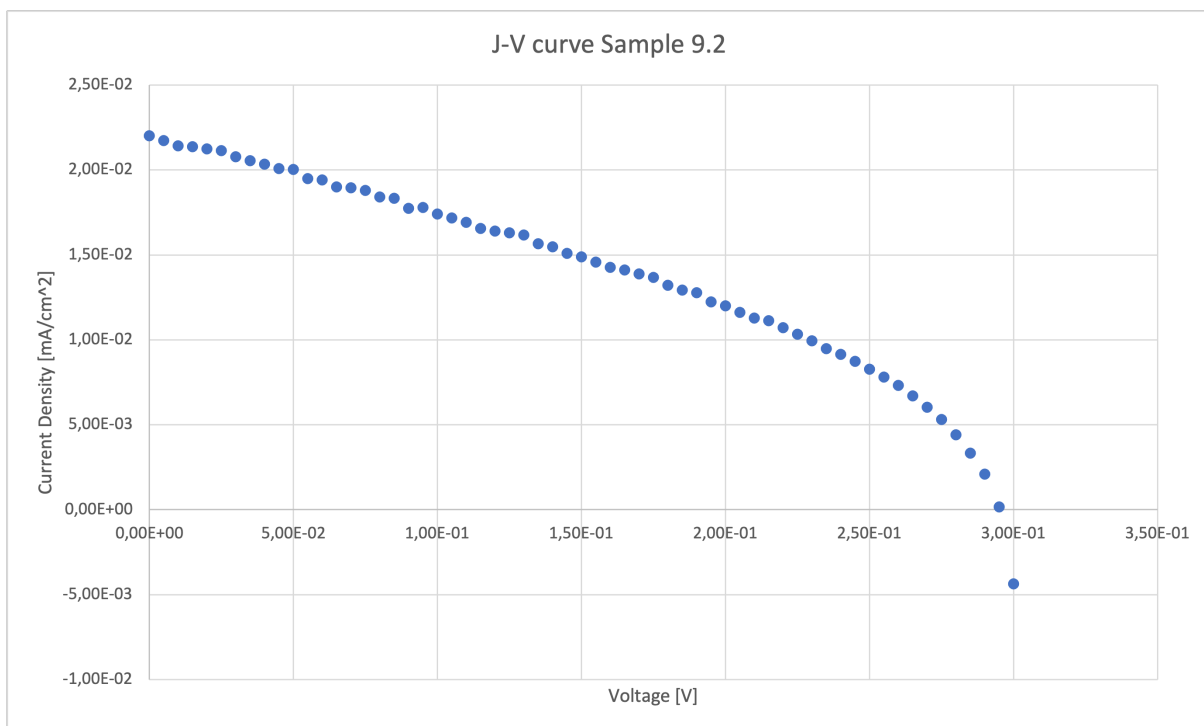


Figure 30: J-V curve from miniature cell 9.2.

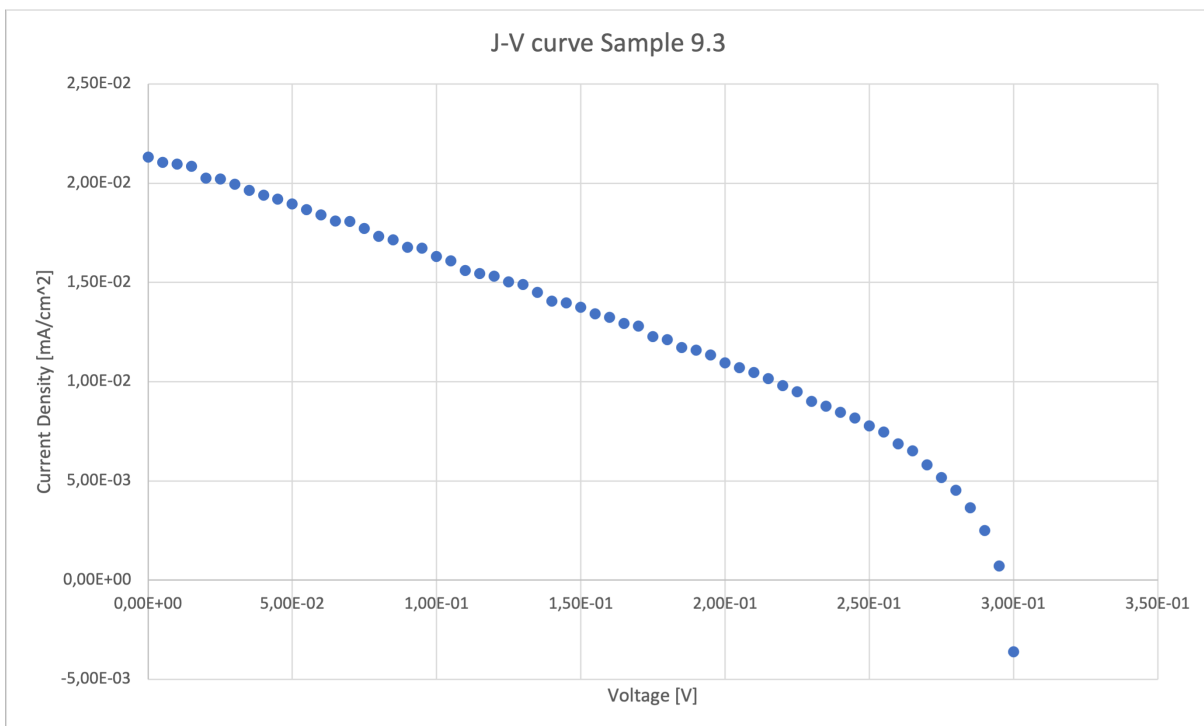


Figure 31: J-V curve from miniature cell 9.3.

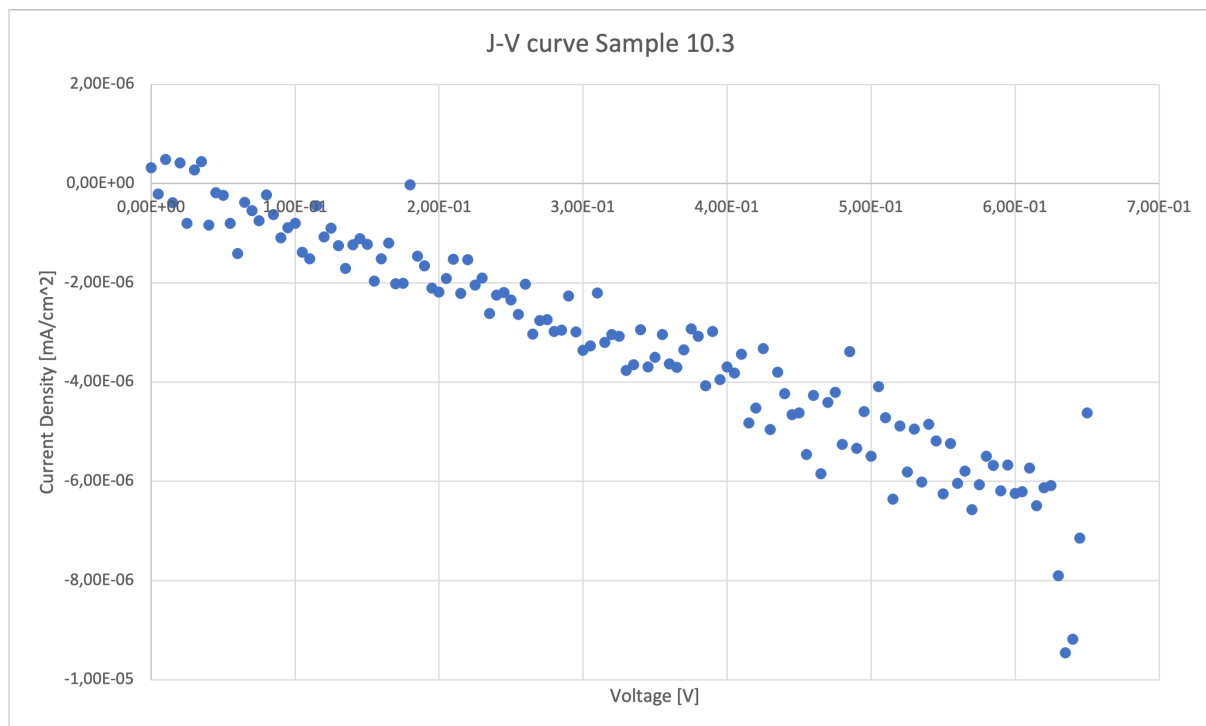


Figure 32: J-V curve from miniature cell 10.3.